Article

Assessing the Impact of Vaccination on the Dynamics of COVID-19 in Africa: A Mathematical Modeling Study

Yvette Montcho [1], Robinah Nalwanga [1], Paustella Azokpota [1], Jonas Têlé Doumatè [1,2], Bruno Enagnon Lokonon [1], Valère Kolawole Salako [1], Martin Wolkewitz [3] and Romain Glèlè Kakaï [1,*]

1 Laboratoire de Biomathématiques et d'Estimations Forestières, Université d'Abomey-Calavi, Cotonou 04 BP 1525, Benin
2 Faculté des Sciences et Techniques, Université d'Abomey-Calavi, Abomey-Calavi, Cotonou 01 BP 526, Benin
3 Institute of Medical Biometry and Statistics, Faculty of Medicine and Medical Center, University of Freiburg, 79104 Freiburg, Germany
* Correspondence: romain.glelekakai@fsa.uac.bj

Abstract: Several effective COVID-19 vaccines are administered to combat the COVID-19 pandemic globally. In most African countries, there is a comparatively limited deployment of vaccination programs. In this work, we develop a mathematical compartmental model to assess the impact of vaccination programs on curtailing the burden of COVID-19 in eight African countries considering SARS-CoV-2 cumulative case data for each country for the third wave of the COVID-19 pandemic. The model stratifies the total population into two subgroups based on individual vaccination status. We use the detection and death rates ratios between vaccinated and unvaccinated individuals to quantify the vaccine's effectiveness in reducing new COVID-19 infections and death, respectively. Additionally, we perform a numerical sensitivity analysis to assess the combined impact of vaccination and reduction in the SARS-CoV-2 transmission due to control measures on the control reproduction number (R_c). Our results reveal that on average, at least 60% of the population in each considered African country should be vaccinated to curtail the pandemic (lower the R_c below one). Moreover, lower values of R_c are possible even when there is a low (10%) or moderate (30%) reduction in the SARS-CoV-2 transmission rate due to NPIs. Combining vaccination programs with various levels of reduction in the transmission rate due to NPI aids in curtailing the pandemic. Additionally, this study shows that vaccination significantly reduces the severity of the disease and death rates despite low efficacy against COVID-19 infections. The African governments need to design vaccination strategies that increase vaccine uptake, such as an incentive-based approach.

Keywords: COVID-19; vaccination impact; compartmental model; reproduction number; Africa

1. Introduction

Coronavirus disease 2019 (COVID-19) caused by severe acute respiratory syndrome coronavirus-2 (SARS-CoV-2) [1] invaded the world unexpectedly in 2019 and changed human life tremendously [2]. The disease outbreak first emerged in Wuhan City, Hubei Province of China [3], and after that, it spread to the United States, Europe, Asia, and later on, to other continents. Despite its rampant spread, studies indicated that the spread of the disease in Africa had not followed an exponential path as for the rest of the world (Europe, United States, Asia), implying that Africa has not yet experienced the predicted heavy disease burden [4]. By the end of November 2022, approximately 12.7 million cases and 257,984 deaths, representing 2.1% and 4.3%, respectively of the global figures, were reported in Africa [5]. In an effort to curb the transmission of SARS-CoV-2, many African countries have implemented non-pharmaceutical interventions (NPIs), such as social distancing, quarantine of suspected infection cases, use of face masks, contact tracing and testing, among others [6]. Several studies [7–9] have investigated the effectiveness of NPIs on the transmission dynamics of COVID-19 using various approaches. Findings from these

studies have indicated that NPIs have been sufficiently effective in mitigating the burden of the pandemic, at least for the first and second waves. However, the emergence of new SARS-CoV-2 variants, which are currently categorized as Variants of Concern (VOC) by the WHO, such as Alpha, Beta, Omicron, and Delta strains [10] have reduced the effectiveness of NPIs, creating the need for more effective control measures such as vaccination [11].

Vaccination against COVID-19 has been identified as one of the most viable options to suppress the SARS-CoV-2 transmission globally [12] and as well achieve herd immunity [13]. Several COVID-19 vaccines have been approved for use, and they are commonly administered as either a single dose such as Johnson & Johnson (52.0–72.0% of efficacy) or two-doses vaccine such as AstraZeneca (62.1–90.0%), Pfizer-BioNTech (95.0%) and Moderna (94.1%) [14,15]. The first mass vaccination program began in early 2020. By the end of November 2022, more than 5.46 billion vaccine doses have been administered worldwide, representing 71.1% of the global population [16]. Over 2.6 million additional doses (boosters) have been administered to fully vaccinated people [16]. COVID-19 vaccination rates remain low in most African countries. As of November 2022, only 33% of the population had received at least one dose of the vaccine compared to the global average of 69.0% [16]. Vaccine hesitancy due to widespread misconceptions and beliefs about vaccines, a lack of adequate infrastructure and logistics to handle vaccination campaigns, and a low-risk perception of the pandemic, notably with the recent decline in cases, are the major barriers to low vaccination uptake in Africa [17,18]. Several clinical trials have shown that COVID-19 vaccines are effective in reducing disease severity and individual symptoms, decreasing fatalities, hospitalizations, and admissions to intensive care units [19,20]. However, the emergence of new variants may outweigh some of these gains. Given the contagious nature of infectious diseases, particularly COVID-19, there is mounting evidence that poor vaccine uptake may not only amplify disease transmission in unvaccinated subpopulations but also heighten the risk for vaccinated populations, especially in situations where vaccines confer imperfect immunity. A recent study by the US Centers for Disease Control and Prevention on an outbreak of COVID-19 in a federal prison in Texas showed an equal transmission rate among vaccinated and unvaccinated individuals [21]. Mathematical models are important tools to describe and predict the spread of epidemics and can be used to quantify the potential impact of vaccination programs on disease dynamics. Currently, several mathematical models have been developed to predict and assess the impact of vaccination on the transmission dynamics of COVID-19 [22–26].

Machado et al. [27] analyzed the impact of vaccination on the control of the pandemic using a simple SEIR-based simulation model. The authors believe that an increased vaccination rate combined with continued adherence to non-pharmaceutical interventions can greatly delay the peak of infection. With the ongoing vaccination program, the trajectory of a pandemic is determined by how the virus spreads in unvaccinated and vaccinated individuals. The effect of mixing vaccinated and unvaccinated populations on the risk of SARS-CoV-2 infection among vaccinated people was investigated in a study by [28] using a basic SIR model. Under all mixing assumptions, their model demonstrated that the risk of infection was significantly higher in the unvaccinated group than in the vaccinated group. However, the author acknowledges that the simplicity of the model does not reflect the real-world process of the pandemic, for instance, demographics, waning of the vaccine, and natural loss of immunity, among others.

Even though various research studies are being conducted in Africa, they largely focus on COVID-19 vaccination prioritization strategies [29–31] or vaccine acceptance [32–34]. To the best of our knowledge, however, studies that use real-world vaccination data to evaluate the impact of COVID-19 vaccination programs on the dynamics of the disease in African countries are still very few [35]. Despite the contributions of these studies, they showed some limitations. Thus, the previous studies ignore the fact that transmission can occur both within vaccinated and unvaccinated people and between vaccinated and unvaccinated people (i.e., an infectious unvaccinated person can infect a vaccinated person and vice versa).

In this study, we developed a mathematical model to quantitatively assess the impact of vaccination programs on the dynamics of COVID-19 in Africa, focusing on eight countries (Algeria, DR Congo, Kenya, Lybia, Namibia, Nigeria, Rwanda, and South Africa), representing the four main regions of the continent. The model was used to (i) assess the impact of vaccination on COVID-19 incidence and mortality in a mixed population of vaccinated and unvaccinated individuals and (ii) evaluate the combined impact of vaccination with different levels of NPIs on the dynamics of COVID-19.

2. Materials and Methods

2.1. Model Formulation

In this study, we developed a deterministic compartmental model of COVID-19 stratified by infection status and vaccination status to describe the impact of an imperfect vaccine on the transmission dynamics of the disease. The proposed model is a modification of a previously developed compartmental model [36] where vaccination was incorporated in the COVID-19 model as a pharmaceutical intervention strategy in South Africa. The mathematical model comprises eight epidemiological states depending on the individual's health and vaccination status. The total population at time t denoted by $N(t)$ is divided into two groups, i.e., unvaccinated and vaccinated, which are represented by subscripts u and v, respectively.

The unvaccinated population denoted by $N(u)$ is further subdivided into eight subpopulations of individuals that are: unvaccinated susceptible ($S_u(t)$), unvaccinated exposed ($E_u(t)$), unvaccinated pre-symptomatic infectious ($I_{p_u}(t)$), unvaccinated asymptomatic infectious ($I_{A_u}(t)$), unvaccinated symptomatic infectious ($I_{S_u}(t)$), the detected infectious unvaccinated via testing ($C_u(t)$), unvaccinated recovered ($R_u(t)$), and unvaccinated deceased $D_u(t)$. Thus, the total population for the unvaccinated is given by:

$$N_u(t) = S_u(t) + E_u(t) + I_{p_u}(t) + I_{A_u}(t) + I_{S_u}(t) + C_u(t) + R_u(t).$$

Similarly, the vaccinated population denoted by $N(v)$ is also further subdivided into eight subpopulations of individuals that are: vaccinated susceptible ($S_v(t)$), vaccinated exposed ($E_v(t)$), vaccinated pre-symptomatic infectious ($I_{p_v}(t)$), vaccinated asymptomatic infectious ($I_{A_v}(t)$), vaccinated symptomatic infectious ($I_{S_v}(t)$), detected infectious vaccinated via testing ($C_v(t)$), vaccinated recovered ($R_v(t)$) and vaccinated deceased $D_v(t)$. The total population for the vaccinated is given by:

$$N_v(t) = S_v(t) + E_v(t) + I_{p_v}(t) + I_{A_v}(t) + I_{S_v}(t) + C_v(t) + R_v(t).$$

Therefore, the total population at time t (denoted by $N(t)$) is

$$N(t) = N_u(t) + N_v(t).$$

When developing the mathematical model, we made some assumptions or comments, which are as follows.

(i)　Vaccination is administered to unvaccinated individuals that are susceptible, exposed, pre-symptomatic, asymptomatic, and naturally recovered from the virus. The model does not consider the vaccination of symptomatic and confirmed infectious individuals.

(ii)　The COVID-19 vaccine administered is imperfect, i.e., it provides only partial protection against COVID-19 infections. Thus, infections for the vaccinated can occur but at a reduced rate compared to that of the unvaccinated susceptible individuals.

(iii)　Both vaccine-derived and natural immunity may wane over time in individuals, implying that individuals rejoin the fully susceptible class after a certain period [36–38].

(iv)　We assume that there is homogeneous mixing among the population, which means that every individual in the community is equally likely to mix and acquire infections from each member when they make contact.

(v) Since the COVID-19 pandemic has persisted for a long time, we include the vital dynamics (birth and natural death) in the model.

We suppose that all the births and the immigration from the population are recruited into the unvaccinated susceptible class at rate Λ. Susceptible unvaccinated individuals become exposed following effective contact with either unvaccinated or vaccinated pre-asymptomatic, asymptomatic, symptomatic, and confirmed infectious individuals at a rate λ_u. After the latent period, the unvaccinated exposed individuals become pre-asymptomatic at a progression rate α_E. At the end of the incubation period, unvaccinated pre-symptomatic infectious individuals either develop clinical symptoms and move to the unvaccinated symptomatic infectious (I_{S_u}) at a rate $\rho_1 \alpha_p$ (where ρ_1 is the probability of developing symptoms), or they continue to show no symptoms and move on to the unvaccinated asymptomatic class (I_{A_u}) at the rate $(1 - \rho_1)\alpha_p$. The asymptomatic and symptomatic unvaccinated infectious individuals are tested and confirmed positive at a detection rate q_{a_1} and q_{s_1}, respectively, and move to the unvaccinated confirmed class (C_u). The symptomatic and confirmed unvaccinated infectious individuals might die due to COVID-19-related complications at the rate δ_{s_1} and δ_{c_1}, respectively. The parameters γ_{a_1}, γ_{s_1} and γ_{c_1} account for the recovery rates for unvaccinated individuals in the asymptomatic, symptomatic and confirmed classes, respectively. The recovered unvaccinated individuals may lose their natural immunity at a rate d_u, and thus, they can become susceptible.

We assume that unvaccinated individuals in the susceptible, exposed, pre-symptomatic, asymptomatic and recovered classes are vaccinated at rate ν. Due to the imperfect vaccine administrated, vaccinated individuals are not immune from infection. The vaccine-induced immunity of the susceptible vaccinated individuals wanes at a per capita rate ω. Hence, after a given time, the susceptible vaccinated population can become infected by the virus when they make contact with either unvaccinated or vaccinated pre-asymptomatic, asymptomatic, symptomatic, and confirmed infectious individuals at a rate λ_v. The population in the class E_v becomes infectious at a rate α_E and moves to the pre-asymptomatic class I_{p_v}. After the pre-asymptomatic period, proportion ρ_2 develops COVID-19 symptoms and moves to the symptomatic infectious class (I_{S_v}), while the rest continue to show no symptoms and move on to the vaccinated asymptomatic class (I_{A_v}). The asymptomatic and symptomatic vaccinated infectious individuals are tested and confirmed positive at a detection rate q_{a_2} and q_{s_2}, respectively, and move to the vaccinated confirmed class (C_v). The symptomatic and confirmed vaccinated infectious individuals may die due to COVID-19-related complications at the rate δ_{s_2} and δ_{c_2}. The parameters γ_{a_2}, γ_{s_2} and γ_{c_2} account for the recovery rates of vaccinated individuals in the asymptomatic, symptomatic and confirmed classes. The recovered vaccinated individuals may lose derived vaccine immunity at a rate d_v, and thus, they can become susceptible. Each subpopulation is reduced by a natural death at a constant rate μ.

The flowchart of the formulated model using all the above assumptions is given in Figure 1. Additionally, all the model state variables and the parameters with their description are presented in Table 1 and Table 2, respectively. Hence, the COVID-19 dynamics for the unvaccinated population are described by the following system of differential equations:

$$
\begin{aligned}
\dot{S}_u &= \Lambda - (\lambda_u + \mu + \nu)S_u + S_v\omega + d_u R_u, \\
\dot{E}_u &= \lambda_u S_u - (\alpha_E + \nu + \mu)E_u, \\
\dot{I}_{P_u} &= \alpha_E E_u - (\alpha_p + \mu + \nu + q_{p_1})I_{P_u}, \\
\dot{I}_{A_u} &= (1 - \rho_1)\alpha_p I_{P_u} - (\mu + \nu + \gamma_{a_1} + q_{a_1})I_{A_u}, \\
\dot{I}_{S_u} &= \rho_1 \alpha_p I_{P_u} - (\mu + \gamma_{s_1} + q_{s_1} + \delta_{s_1})I_{S_u}, \\
\dot{C}_u &= q_{a_1} I_{A_u} + q_{s_1} I_{S_u} + q_{p_1} I_{P_u} - (\delta_{c_1} + \gamma_{c_1} + \mu)C_u, \\
\dot{D}_u &= \delta_{s_1} I_{S_u} + \delta_{c_1} C_u, \\
\dot{R}_u &= \gamma_{a_1} I_{A_u} + \gamma_{s_1} I_{S_u} + \gamma_{c_1} C_u - (d_u + \mu + \nu)R_u,
\end{aligned}
\tag{1}
$$

where λ_u is the force of infection for the unvaccinated individuals, which is defined by:

$$\lambda_u = \frac{b_{uu}(\theta_{P_u} I_{P_u} + \theta_{A_u} I_{A_u} + \theta_{s_u} I_{S_u} + \theta_{c_u} C_u)(1 - \psi_u)}{N},$$
$$+ \frac{b_{uv}(\theta_{P_v} I_{P_v} + \theta_{A_v} I_{A_v} + \theta_{S_v} I_{S_v} + \theta_{c_v} C_v)(1 - \psi_v)}{N}.$$

Similarly, using the same model assumptions and parameter description, the COVID-19 dynamics for the vaccinated population are described by the following system of differential equations:

$$
\begin{aligned}
\dot{S}_v &= \nu S_u + d_v R_v - (\lambda_v + \mu + \omega)S_v, \\
\dot{E}_v &= \nu E_u + \lambda_v S_v - (\alpha_E + \mu)E_v, \\
\dot{I}_{P_v} &= \nu I_{P_u} + \alpha_E E_v - (\alpha_p + q_{p_2} + \mu) I_{P_v}, \\
\dot{I}_{A_v} &= \nu I_{A_u} + (1 - \rho_2)\alpha_p I_{P_v} - (\mu + \gamma_{a_2} + q_{a_2}) I_{a_v}, \\
\dot{I}_{S_v} &= \rho_2 \alpha_p I_{P_v} - (\mu + \gamma_{s_2} + q_{s_2} + \delta_{s_2}) I_{S_v}, \\
\dot{C}_v &= q_{a_2} I_{A_v} + q_{s_2} I_{S_v} + q_{p_2} I_{P_v} - (\delta_{c_2} + \gamma_{c_2} + \mu)C_v, \\
\dot{D}_v &= \delta_{s_2} I_{S_v} + \delta_{c_2} C_v, \\
\dot{R}_v &= \nu R_u + \gamma_{a_2} I_{A_v} + \gamma_{s_2} I_{S_v} + \gamma_{c_2} C_v - (d_v + \mu)R_v,
\end{aligned}
\tag{2}
$$

where λ_v is the force of infection for the vaccinated individuals, which is defined by;

$$\lambda_v = \frac{b_{vu}(\theta_{P_u} I_{P_u} + \theta_{A_u} I_{A_u} + \theta_{S_u} I_{S_u} + \theta_{c_u} C_u)(1 - \psi_u)}{N},$$
$$+ \frac{b_{vv}(\theta_{P_v} I_{P_v} + \theta_{A_v} I_{A_v} + \theta_{S_v} I_{S_v} + \theta_{c_v} C_v)(1 - \psi_v)}{N},$$

where $0 < \psi_u < 1$ and $0 < \psi_v < 1$ represent the percentage decrease in the transmission rate due to control measures among the unvaccinated and vaccinated individuals, respectively.
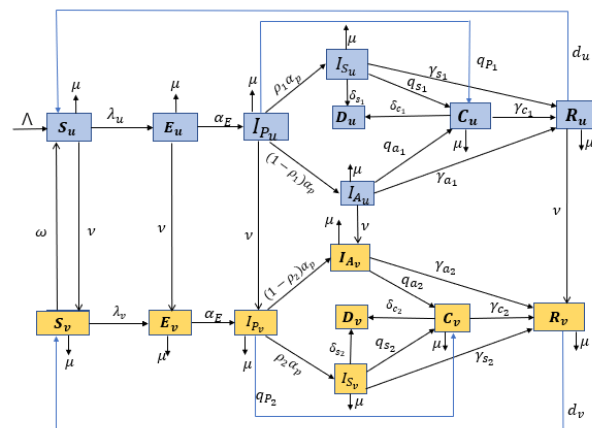
Figure 1. Flowchart of the formulated model.

Table 1. State variables and their description.

State Variable	Description
$S_u(S_v)$	Susceptible unvaccinated (vaccinated) population
$E_u(E_v)$	Exposed unvaccinated (vaccinated) population
$I_{p_u}(I_{p_v})$	Pre-symptomatic infectious unvaccinated (vaccinated) population
$I_{A_u}(I_{A_v})$	Asymptomatic infectious unvaccinated (vaccinated) population
$I_{S_u}(I_{S_v})$	Symptomatic infectious unvaccinated (vaccinated) population
$C_u(C_v)$	Confirmed infectious unvaccinated (vaccinated) population
$R_u(R_v)$	Recovered unvaccinated (vaccinated) population
$D_u(D_v)$	COVID-deceased unvaccinated (vaccinated) population

Table 2. Description of the fixed and estimated model parameters.

Parameter	Description	Unit
Λ	Recruitment rate	Individual day^{-1}
μ	Natural death rate	day^{-1}
ν	Vaccination rate	day^{-1}
ω	Vaccine-derived immunity rate	day^{-1}
$1/\alpha_E$	Latent period	days
$1/\alpha_p$	Pre-symptomatic period	days
d_u (d_v)	Rate at which recovered unvaccinated (vaccinated) individuals from COVID-19 lose acquired immunity	day^{-1}
$\rho_1(\rho_2)$	Proportion of pre-symptomatic infectious unvaccinated (vaccinated), who develop COVID-19 symptoms	dimensionless
b_{ij}	Infection probability of a susceptible individual in class i by an infectious individual in class j, for $(i, j \in u, v)$	dimensionless
$\delta_{s_1}(\delta_{s_2})$	COVID-19 death rate of symptomatic infectious unvaccinated (vaccinated) individuals	day^{-1}
$\delta_{c_1}(\delta_{c_2})$	COVID-19 death rate of confirmed infectious unvaccinated (vaccinated) individuals	day^{-1}
$\gamma_{a_1}(\gamma_{a_2})$	Recovery rate of asymptomatic unvaccinated (vaccinated) individuals	day^{-1}
$\gamma_{s_1}(\gamma_{s_2})$	Recovery rate of symptomatic unvaccinated (vaccinated) individuals	day^{-1}
$\gamma_{c_1}(\gamma_{c_2})$	Recovery rate of symptomatic unvaccinated (vaccinated) individuals	day^{-1}
$\theta_{p_u}(\theta_{A_u}, \theta_{S_u}, \theta_{C_u})$	Relative infectiousness of unvaccinated pre-symptomatic (asymptomatic, symptomatic, confirmed) individuals	dimensionless
$\theta_{p_v}(\theta_{A_v}, \theta_{S_v}, \theta_{C_v})$	Relative infectiousness of unvaccinated pre-symptomatic (asymptomatic, symptomatic, confirmed) individuals	dimensionless
$q_{p_1}(q_{a_1}, q_{s_1})$	Per capita rate at which unvaccinated individuals from the pre-symptomatic (asymptomatic, symptomatic) infectious class test positive	day^{-1}
$q_{p_2}(q_{a_2}, q_{s_2})$	Per capita rate at which vaccinated individuals from the pre-symptomatic (asymptomatic, symptomatic) infectious class test positive	day^{-1}
$\delta_{s_1}(\delta_{s_2})$	COVID-19 induced death rate of unvaccinated (vaccinated) symptomatic infectious individuals	day^{-1}
$\delta_{c_1}(\delta_{c_2})$	COVID-19 induced death rate of unvaccinated (vaccinated) confirmed infectious individuals	day^{-1}

2.2. Data

Five countries per African region were randomly selected among those for which COVID-19 data are available. However, during the modeling process, two countries, namely Benin and Gabon, were excluded due to the poor quality of the data. Consequently, eight African countries, namely, DR Congo, Rwanda, Kenya, Algeria, Libya, Namibia, South Africa, and Nigeria, were selected for analysis in this study. Data on the daily COVID-19 cases, cumulative confirmed cases, and vaccination (number of individuals vaccinated with at least one dose) for each selected country were obtained from COVID-19 data respiratory by Our World in Data (https://github.com/owid/covid-19-data/tree/master/public/data, accessed on 15 july 2022).

The country-specific demographic data such as birth rates and death rates were obtained from the Worldbank via (https://data.worldbank.org/indicator/SP.DYN.CBRT.IN, accessed on 15 july 2022), while data on annual net migration and life expectancy for each country were obtained from Worldmeter, which was available via (https://www.worldometers.info/world-population/population-by-country/, accessed on 15 july 2022).

2.3. Model Fitting and Parameter Estimation Procedure

In this subsection, a single model with sixteen compartments was used for the calibration. We consider a mixed population where both vaccinated and unvaccinated individuals interact, and the transition from the unvaccinated classes to the vaccinated classes is described by some parameters. Thus, we estimated the best values of unknown parameters in models (1–2). We used the data of COVID-19 cumulative cases for each country from the first day of vaccination to the end of the third pandemic wave (end of November 2021). The choice for cumulative case data over daily case data is because it mitigates the effect of re-

porting errors in modeling COVID-19 dynamics. The start dates and the end dates for each country are presented in Table A1. The fixed parameters used in the model-fitting process were obtained from the literature as presented in Table A2, while other fixed parameters that vary per country were calculated and are presented in Table A3.

We define a vaccinated individual as one who has received at least one dose of the COVID-19 vaccine since the available data only give the new vaccination doses delivered per day and make no distinction between the first and second doses. The vaccination rate, ν, for each country is given by

$$\nu = \frac{\text{Vaccine coverage}}{\text{Vaccination period}},$$

where vaccine coverage is the proportion of individuals vaccinated with at least one dose of the COVID-19 vaccine at the end date for each country.

Two demographic parameters were computed for each country, i.e., daily recruitment rate (Λ) of unvaccinated susceptible (through births and net migrations) per (individuals/day) and the natural death rate (μ) per day were computed.

The daily recruitment rate, Λ for each country, was computed using the following expression [39].

$$\Lambda = \frac{r_b \bar{N}}{L}, \tag{3}$$

where $r_b = \chi_p + \frac{A_I}{\bar{N}}$, L is the vaccination time period for each country, χ_p represents the annual births during the vaccination period, L for each country, $\bar{N}$ is the average population size during the vaccination period, L in each country and A_I represents the net annual migration in the country during vaccination period L. Let us take the example of Rwanda. The start date (the first day of vaccination) in Rwanda was 5 March 2021 , and the end date is 13 December 2021 (which corresponds to the last day of the third wave of the pandemic). Thus, the vaccination period considered is $L = 284$ days. The mean total population of Rwanda as of 13 December 2021 is $\bar{N} = 13,461,888$. Using the annual birth rate ($30.725/1000$) and the net annual migration (-9000 individuals) in Rwanda, we obtained the rates $r_b = (30.725/1000) - (9000/\bar{N}) = 0.030056$. Using Equation (3), we computed $\Lambda = 1427.7060$ individuals/day. For each country, the natural death rate of individuals per day was calculated as the reciprocal of the life expectancy (L.E) at the end date (last day of the third wave of the pandemic). For example, in Rwanda, as of 13 December 2021, the average annual life expectancy was L.E = 70 years, then, the natural death rate was $\mu = 1/(70 \times 365)$, which gives $\mu = 3.9112 \times 10^{-5}$ day $^{-1}$.

To find the best set of parameters and initial conditions for each country, we used the nonlinear least square technique in Matlab (2021) with *fminsearchbnd*, which is a built-in Matlab function. Here, we minimize the root mean square of squared differences between each observed cumulative case data and the corresponding cumulative case obtained from the model (RMSE1). We repeated this procedure 2000 times to increase the precision of the estimation.

The value for S_{v0} for each country was obtained from the vaccination data, corresponding to the total number of people vaccinated on the first day of vaccination, such that $S_{v0} = N_{v0}$. We suppose that on the first day of vaccination, no individuals are infected with COVID-19 and vaccinated. Then, we set $E_v = I_{p_v} = I_{A_v} = I_{s_v} = C_v = R_v = D_v = 0$. The solutions to the model Equations (1) and (2) were obtained using the built-in function *ODE45* of Matlab. We used the cross-validation technique for parameter estimation to improve the prediction power of the model. To do this, we divided the data into training (90%) and testing (10%) datasets and computed the root mean square error, RMSE1 (computed using the training dataset) and RMSE2 (using the testing dataset), respectively. The whole model was repeated about 100 times, and the final values of the estimates were those with the smallest value for RMSE2 and RMSE1. We also obtained the 95% confidence interval for the estimated parameters considering the normal distribution. The values

for initial conditions and the corresponding estimated parameters and their 95% CI are presented in Tables A4–A6, respectively.

A numerical simulation was carried out to evaluate the impact of vaccination on COVID-19 incidence and mortality in the selected African countries. To quantify the vaccine impact, we determined the vaccine effectiveness in terms of the detection and death rates ratio for vaccinated individuals in relation to unvaccinated, respectively.

Additionally, numerical sensitivity analysis was performed to assess the combined impact of vaccination with different levels of adherence to non-pharmaceutical interventions (NPIs) on the control reproduction number (R_c). The combined impact was assessed by generating contour plots of control reproduction number (R_c) as a function of vaccine coverage (VC) and control measures (ψ) among both unvaccinated and vaccinated. We suppose that the implementation and lifting of NPIs are related to changes in the transmission rate. We considered varying levels (0 to 1) of adherence to NIPs by both vaccinated and unvaccinated individuals to represent behaviors that reduce the transmission of the SARS-CoV-2 virus. The level of NPI intensity was categorized as follows: low level (self-protection, use of face masks, hand hygiene, and social distancing), moderate level (mobility limitation), and high level (imposition of lockdown, closure of schools, workplaces, churches, etc.). The levels of NPIs adherence among vaccinated and unvaccinated individuals were quantified as low (10%), moderate (30%), and high (50%).

3. Results

3.1. Analytical Results

3.1.1. Computation of Control Reproduction Number

To assess if the implemented control measures, such as vaccination and NPIs, are effective in controlling the COVID-19 outbreak, we computed the control reproduction number, R_c. The control reproduction number is the average number of COVID-19 secondary infections generated by a single infectious individual when introduced in a mixed population of vaccinated and unvaccinated individuals. We used the next-generation approach as described by Diekmann et al. [40] to compute the control reproduction number of our model.

Let us first define the disease-free equilibrium (DFE) of model (1) and (2). At DFE, we have

$E_u = I_{p_u} = I_{A_u} = I_{s_u} = C_v = R_u = D_u = E_v = I_{p_v} = I_{A_v} = I_{s_v} = C_v = R_v = D_v = 0$; $\lambda_u = \lambda_v = 0$; $\dot{S}_u > 0$ and $\dot{S}_v > 0$.

Hence, the disease-free equilibrium point of our model is given by

$$X_0 = (S_u^0, 0, 0, 0, 0, 0, 0, 0, S_v^0, 0, 0, 0, 0, 0, 0, 0)$$

where $S_u^0 = \frac{\Lambda(\mu+\omega)}{\mu(\mu+\omega+\nu)}$,   and $S_v^0 = \frac{\Lambda\nu}{\mu(\mu+\omega+\nu)}$.

Let $X = (E_u, I_{p_u}, I_{A_u}, I_{s_u}, C_u, E_v, I_{p_v}, I_{A_v}, I_{s_v}, C_v)^T$ be a vector of infected classes.

- Let $\mathcal{F}$ be a column vector for all new infections and $F = \Im\mathcal{F}$ be the jacobian of $\mathcal{F}$ at disease-free equilibrium, X_0

$$
\mathcal{F} = \begin{pmatrix} S_u\lambda_u \\ 0 \\ 0 \\ 0 \\ 0 \\ S_v\lambda_v \\ 0 \\ 0 \\ 0 \\ 0 \end{pmatrix} \quad \text{and} \quad F = \begin{pmatrix} 0 & A_1 & A_2 & A_3 & A_4 & 0 & A_5 & A_6 & A_7 & B_8 \\ 0 & 0 & 0 & 0 & 0 & 0 & 0 & 0 & 0 & 0 \\ 0 & 0 & 0 & 0 & 0 & 0 & 0 & 0 & 0 & 0 \\ 0 & 0 & 0 & 0 & 0 & 0 & 0 & 0 & 0 & 0 \\ 0 & 0 & 0 & 0 & 0 & 0 & 0 & 0 & 0 & 0 \\ 0 & B_1 & B_2 & B_3 & B_4 & 0 & B_5 & B_6 & B_7 & B_8 \\ 0 & 0 & 0 & 0 & 0 & 0 & 0 & 0 & 0 & 0 \\ 0 & 0 & 0 & 0 & 0 & 0 & 0 & 0 & 0 & 0 \\ 0 & 0 & 0 & 0 & 0 & 0 & 0 & 0 & 0 & 0 \\ 0 & 0 & 0 & 0 & 0 & 0 & 0 & 0 & 0 & 0 \end{pmatrix}
$$

where

$$A_1 = \frac{S_u^0 b_{uu}\theta_{P_u}(1-\psi_u)}{N} \quad A_2 = \frac{S_u^0 b_{uu}\theta_{A_u}(1-\psi_u)}{N} \quad A_3 = \frac{S_u^0 b_{uu}\theta_{s_u}(1-\psi_u)}{N}$$

$$A_4 = \frac{S_u^0 b_{uu}\theta_{c_u}(1-\psi_u)}{N} \quad A_5 = \frac{S_u^0 b_{vu}\theta_{pv}(1-\psi_u)}{N} \quad A_6 = \frac{S_u^0 b_{vu}\theta_{c_v}(1-\psi_u)}{N}$$

$$A_7 = \frac{S_u^0 b_{vu}\theta_{s_v}(1-\psi_u)}{N} \quad A_8 = \frac{S_u^0 b_{vu}\theta_{c_v}(1-\psi_u)}{N}$$

$$B_1 = \frac{S_v^0 b_{uv}\theta_{P_v}(1-\psi_v)}{N} \quad B_2 = \frac{S_v^0 b_{uv}\theta_{A_v}(1-\psi_v)}{N} \quad B_3 = \frac{S_v^0 b_{uv}\theta_{S_u}(1-\psi_v)}{N}$$

$$B_4 = \frac{S_v^0 b_{uv}\theta_{C_v}(1-\psi_v)}{N} \quad B_5 = \frac{S_v^0 b_{vv}\theta_{P_v}(1-\psi_v)}{N} \quad B_6 = \frac{S_v^0 b_{vv}\theta_{A_v}(1-\psi_v)}{N}$$

$$B_7 = \frac{S_v^0 b_{vv}\theta_{S_v}(1-\psi_v)}{N} \quad B_8 = \frac{S_v^0 b_{vv}\theta_{C_v}(1-\psi_v)}{N}$$

- Let $\mathcal{V}$ be the matrix of net transitions

$$
\mathcal{V} = \begin{pmatrix} (\alpha_E + \nu + \mu)E_u \\ -\alpha_E E_u + (\alpha_P + \mu + \nu)I_{P_u} \\ -(1-\rho_1)\alpha_P I_{P_u} + (\mu + \nu + \gamma_{a_1} + q_{a_1})I_{A_u} \\ -\rho_1\alpha_P I_{P_u} + (\mu + \gamma_{s_1} + q_{s_1} + \delta_{s_1})I_{S_u} \\ -q_{a_1}I_{A_u} - q_{s_1}I_{S_u} + (\delta_{c_1} + \gamma_{c_1} + \mu)C_u \\ -\nu E_u + (\alpha_E + \mu)E_v \\ -\nu I_{P_u} - \alpha_E E_v + (\alpha_P + \mu)I_{P_v} \\ -\nu I_{A_u} - (1-\rho_2)\alpha_P I_{P_v} + (\mu + \gamma_{a_2} + q_{a_2})I_{a_v} \\ -\rho_2\alpha_P I_{P_v} - (\mu + \gamma_{s_2} + q_{s_2} + \delta_{s_2})I_{S_v} \\ -q_{a_2}I_{A_v} - q_{s_2}I_{S_v} + (\delta_{c_2} + \gamma_{c_2} + \mu)C_v \end{pmatrix}
$$

- The Jacobian matrix ($V = \Im\mathcal{V}$) of matrix V, at disease-free equilibrium, X_0 is given as:

$$
V = \begin{pmatrix}
a_1 & 0 & 0 & 0 & 0 & 0 & 0 & 0 & 0 & 0 \\
-\alpha_E & a_2 & 0 & 0 & 0 & 0 & 0 & 0 & 0 & 0 \\
0 & -\alpha_p(1-\rho_1) & a_3 & 0 & 0 & 0 & 0 & 0 & 0 & 0 \\
0 & -\alpha_p\rho_1 & 0 & a_4 & 0 & 0 & 0 & 0 & 0 & 0 \\
0 & -q_{p_1} & -q_{a_1} & -q_{s_1} & a_5 & 0 & 0 & 0 & 0 & 0 \\
-\nu & 0 & 0 & 0 & 0 & a_6 & 0 & 0 & 0 & 0 \\
0 & -\nu & 0 & 0 & 0 & -\alpha_E & a_7 & 0 & 0 & 0 \\
0 & 0 & 0 & -\nu & 0 & 0 & -\alpha_p(1-\rho_2) & a_8 & 0 & 0 \\
0 & 0 & 0 & 0 & 0 & 0 & -\alpha_p\rho_2 & 0 & a_9 & 0 \\
0 & 0 & 0 & 0 & 0 & 0 & -q_{p2} & -q_{a2} & -q_{s2} & a_0
\end{pmatrix}
$$

where

$$
\begin{aligned}
&a_1 = \alpha_E + \mu + \nu && a_2 = \alpha_p + \mu + \nu + q_{p1} && a_3 = \alpha_p + \mu + \nu + q_{p1} \\
&a_4 = \gamma_{a1} + \mu + \nu + q_{a1} && a_5 = \gamma_{c1} + \mu + \delta_{c1} && a_6 = \alpha_E + \mu \\
&a_7 = \alpha_p + \mu + q_{p2} && a_8 = \gamma_{a2} + \mu + q_{a2} && a_9 = \delta_{s2} + \gamma_{s2} + \mu + q_{s2} \\
&a_0 = \gamma_{c2} + \mu + \delta_{c2}.
\end{aligned}
$$

Using the next-generation matrix approach, the control reproduction number R_c of the model is computed as the spectral radius $\rho\left(F \times V^{-1}\right)$ of the next generation matrix $F \times V^{-1}$, i.e.

$$
R_c = \rho\left(F \times V^{-1}\right).
$$

The expression for the control reproduction number, R_c, is the sum of three quantities, i.e.,

$$
R_c = R_{c1} + R_{c2} + R_{c3}, \tag{4}
$$

where quantities R_{c1} and R_{c2} are contributions of the unvaccinated and vaccinated infectious classes, respectively, while R_{c3} is the contribution from the interaction between the vaccinated and unvaccinated infectious classes to the control reproduction number.

The component R_{c_1} is the sum of the four components, i.e., $R_{c_{1Pu}}$, $R_{c_{1Au}}$, $R_{c_{1Su}}$, and $R_{c_{1Cu}}$, which represent the contribution of the pre-asymptomatic, asymptomatic, symptomatic, and confirmed infectious unvaccinated classes, respectively.

$$
R_{c_1} = R_{c_{1Pu}} + R_{c_{1Au}} + R_{c_{1Su}} + R_{c_{1Cu}}, \tag{5}
$$

where

$$
R_{c_{1Pu}} = \frac{\alpha_E S_u^0 b_{uu}(1 - \psi_u)\theta_{P_u}}{2N^0 a_1 a_2},
$$

$$
R_{c_{1Au}} = \frac{\alpha_E S_u^0 b_{uu}(1 - \psi_u)\alpha_p(1 - \rho_1)\theta_{A_u}}{2N^0 a_1 a_2 a_3},
$$

$$
R_{c_{1Su}} = \frac{\alpha_E S_u^0 b_{uu}(1 - \psi_u)\alpha_p \rho_1 \theta_{S_u}}{2N^0 a_1 a_2 a_4},
$$

$$
R_{c_{1Cu}} = \frac{\alpha_E S_u^0 b_{uu}(1 - \psi_u)\left[a_3 a_4 + a_4 q_{a_1}\alpha_p(1 - \rho_1) + a_3 q_{s_1}\rho_1\right]\theta_{C_u}}{2N^0 a_1 a_2 a_3 a_4 a_5},
$$

N^0 is the initial population at disease-free equilibrium and is given by $N^0 = S_u^0 + S_v^0$.

Similarly, the component R_{c_2} is the sum of the four components, i.e., $R_{c_{2Pv}}$, $R_{c_{2Av}}$, $R_{c_{2Sv}}$, and $R_{c_{2Cv}}$, which represent the contribution of the pre-asymptomatic, asymptomatic, symptomatic, and confirmed infectious vaccinated individuals, respectively.

$$
R_{c_2} = R_{c_{2Pv}} + R_{c_{2Av}} + R_{c_{2Sv}} + R_{c_{2Cv}}, \tag{6}
$$

$$
R_{c_{2Pv}} = \frac{\alpha_E S_v^0 b_{vv}(1 - \psi_v)\theta_{P_v}}{2N^0 a_6 a_7},
$$

$$
R_{c_{2Av}} = \frac{\alpha_E S_v^0 b_{vv}(1 - \psi_v)\alpha_p(1 - \rho_2)\theta_{A_v}}{2N^0 a_6 a_7 a_8},
$$

$$
R_{c_{2Sv}} = \frac{\alpha_E S_v^0 b_{vv}(1 - \psi_v)\alpha_p \rho_2 \theta_{S_v}}{N^0 a_6 a_7 a_9},
$$

$$
R_{c_{2Cu}} = \frac{\alpha_E S_v^0 b_{vv}(1 - \psi_v)\left[a_8(a_9 q_{p_2} + q_{s_2}\alpha_p \rho_2) + a_9 q_{a_2}\alpha_p(1 - \rho_2)\right]\theta_{C_v}}{2N^0 a_0 a_6 a_7 a_8 a_9}.
$$

The quantity, R_{c_3} is also defined as;

$$R_{c_3} = R_{c_{1V}} + \sqrt{[R_{c_1} + R_{c_{1V}} - R_{c_2}]^2 + \frac{4}{m_2}(m_1 R_{c_1} + m_2 R_{c_{1V}})},$$

where

$R_{c_{1V}} = R_{c_{1P_v}} + R_{c_{1A_v}} + R_{c_{1S_v}} + R_{c_{1C_v}}$, $\quad m_1 = \frac{b_{vu}}{b_{uu}}$, $\quad$ and $\quad m_2 = \frac{b_{vv}}{b_{uv}}$.

We define $R_{c_{1V}}$ as the sum of four components, i.e., $R_{c_{1P_v}}, R_{c_{1A_v}}, R_{c_{1S_v}}$, and $\quad R_{c_{1C_v}}$, which represent the contribution from the interaction of the unvaccinated individuals with the pre-asymptomatic, symptomatic, and confirmed infectious vaccinated individuals.

$$R_{c_{1P_v}} = \frac{\alpha_E \nu S_u^0 b_{uv}(1-\psi_v)\theta_{P_v}}{2N^0 a_1 a_2 a_6 a_7},$$

$$R_{c_{1A_v}} = \frac{\alpha_E \nu S_u^0 b_{uv}(1-\psi_v)[a_3(1-\rho_2)(a_2+a_6+a_6 a_7(1-\rho_1))]\theta_{A_v}}{2N^0 a_1 a_2 a_3 a_6 a_7 a_8},$$

$$R_{c_{1S_v}} = \frac{\alpha_E \nu S_u^0 b_{uv}(1-\psi_v)\alpha_p \rho_2(a_2+a_6)\theta_{S_v}}{2N^0 a_1 a_2 a_6 a_7 a_9},$$

$$R_{c_{1C_v}} = \frac{\alpha_E \nu S_u^0 b_{uv}(1-\psi_v)\left[a_3(a_2+a_6)\left(a_8(a_9 q_{p_2}+\alpha_P q_{s_2}\rho_2)+a_9 \alpha_P q_{a_2}(1-\rho_2)\right)+D\right]\theta_{C_v}}{2N^0 a_0 a_1 a_2 a_3 a_6 a_7 a_8 a_9}$$

where $D = a_9 a_6 a_7 q_{a_2} \alpha_P(1-\rho_1)$.

3.1.2. Computation of Basic Reproduction Number

In the absence of vaccination and non-pharmaceutical interventions, the control reproduction number reduces to the basic reproduction number, denoted by R_0, which is given by

$$R_{0c} = \mathcal{R}_c|S_v^0 = \nu = \psi_u = \psi_v = 0.$$

The expression for the basic reproduction number, R_{c_0}, is the sum of two quantities since in the absence of vaccination $S_v^0 = 0$, then $R_{0c2} = 0$.

$$R_{0c} = R_{0c1} + R_{0c3}, \tag{7}$$

where quantities R_{0c1} represent the contribution of the unvaccinated infectious classes while R_{0c3} is a contribution from the interaction between the vaccinated and unvaccinated infectious classes to the basic reproduction number.

The component, R_{0c1} is the sum of the four components, i.e., $R_{0c_{1Pu}}, R_{0c_{1Au}}, R_{0c_{1Su}}$, and $\quad R_{0c_{1Cu}}$, which represent the contribution of the pre-asymptomatic, asymptomatic, symptomatic, and confirmed infectious unvaccinated classes, respectively.

$$R_{0c1} = R_{0c_{1Pu}} + R_{0c_{1Au}} + R_{0c_{1Su}} + R_{0c_{1Cu}}, \tag{8}$$

where

$$R_{0c_{1Pu}} = \frac{\alpha_E b_{uu} \theta_{Pu}}{2(\alpha_E + \mu)(\alpha_p + \mu + q_{p1})},$$

$$R_{0c_{1Au}} = \frac{\alpha_E \alpha_p b_{uu} \theta_{Au}(1 - p_1)}{2(\alpha_E + \mu)(\alpha_p + \mu + q_{p1})(\gamma_{a1} + \mu + q_{a1})},$$

$$R_{0c_{1Su}} = \frac{\alpha_E \alpha_p b_{uu} \rho_1 \theta_{3u}}{2a_4(\alpha_E + \mu)(\alpha_p + \mu + q_{p1})},$$

$$R_{0c_{1Cu}} = \frac{\alpha_E b_{uu} \theta_{Cu}(\alpha_p q_{a1}(1 - \rho_1)a_4 + q_{p1}(\gamma_{a1} + \mu + q_{a1})a_4 + q_{s1}\rho_1(\gamma_{a1} + \mu + q_{a1}))}{2a_5 a_4(\alpha_E + \mu)(\alpha_P + \mu + q_{p1})(\delta_{c1} + \gamma_{c1} + \mu)}.$$

The quantity, R_{0c3} is also defined as:

$$R_{0c3} = \sqrt{R_{0c1}^2 + \frac{4}{m_2}(m_1 R_{0c1})}.$$

3.2. Numerical Results

Results from the model fitting show a good match between the number of cumulative confirmed cases from the data (red curve) and the number of cumulative confirmed cases obtained from the model (blue curve) for the eight selected countries shown in Figure A1.

3.2.1. Dynamics of COVID-19 Infectious Classes Over Time

We explore how infectious class populations evolve over time with an imperfect vaccine. The estimated model parameters presented in Tables A5 and A6 were used to compute the ratio of the number of breakthrough infections that would arise among the vaccinated in relation to the unvaccinated subpopulations for the four infectious classes. Figure 2 shows the evolution of the ratio of infected vaccinated individuals to the number of infected unvaccinated for each infectious class (pre-symptomatic, asymptomatic, symptomatic, and confirmed) for the considered countries. Since the COVID-19 vaccines provide partial protection coupled with the emergence of new variants of concern, many breakthrough infections have been reported in most African countries.

Overall, the computed ratios for all eight countries are less than one (varying from 0 to 0.5), indicating that the number of breakthrough infections that arise from the vaccinated infectious classes is relatively lower than that for the unvaccinated. Rwanda and Algeria have the highest ratios, while DR Congo has the least computed ratios (Figure 2).

Results also demonstrated that the ratio of pre-symptomatic and asymptomatic infected individuals increases as the vaccination period increases. For example, in August 2021, the number of vaccinated asymptomatic individuals in Rwanda was 0.28 times that of the unvaccinated. However, this ratio increased to 0.45 by the end of November 2021 (Figure 2). This shows that the proportion of undetected cases (i.e. pre-symptomatic and asymptomatic) for both vaccinated and unvaccinated are generally high in all the African countries as indicated by the blue and red lines (Figure 2).

For all countries, the symptomatic infections among the vaccinated and unvaccinated, except for South Africa, exhibit parallel trends over time. This implies no significant difference in the number of primary infections from unvaccinated and breakthrough infections from the vaccinated symptomatic class, thus demonstrating the vaccine's effectiveness in reducing the number of both vaccinated and unvaccinated individuals who develop COVID-19 symptoms.

Countries such as Algeria, Namibia, and Libya have similar parallel trends for confirmed and symptomatic cases. The findings from Figure 2 show that DR Congo has the least computed ratios for the four infectious classes due to the low vaccine coverage.

For instance, the computed ratio for the number of vaccinated confirmed individuals to unvaccinated is ≈0.0001 as of November 2021. This means that the number of vaccinated individuals confirmed positive for COVID-19 is ≈0. Notably, the number of breakthrough infections from the confirmed vaccinated individuals was higher in countries such as Rwanda, Kenya, South Africa, and Algeria than in other countries.
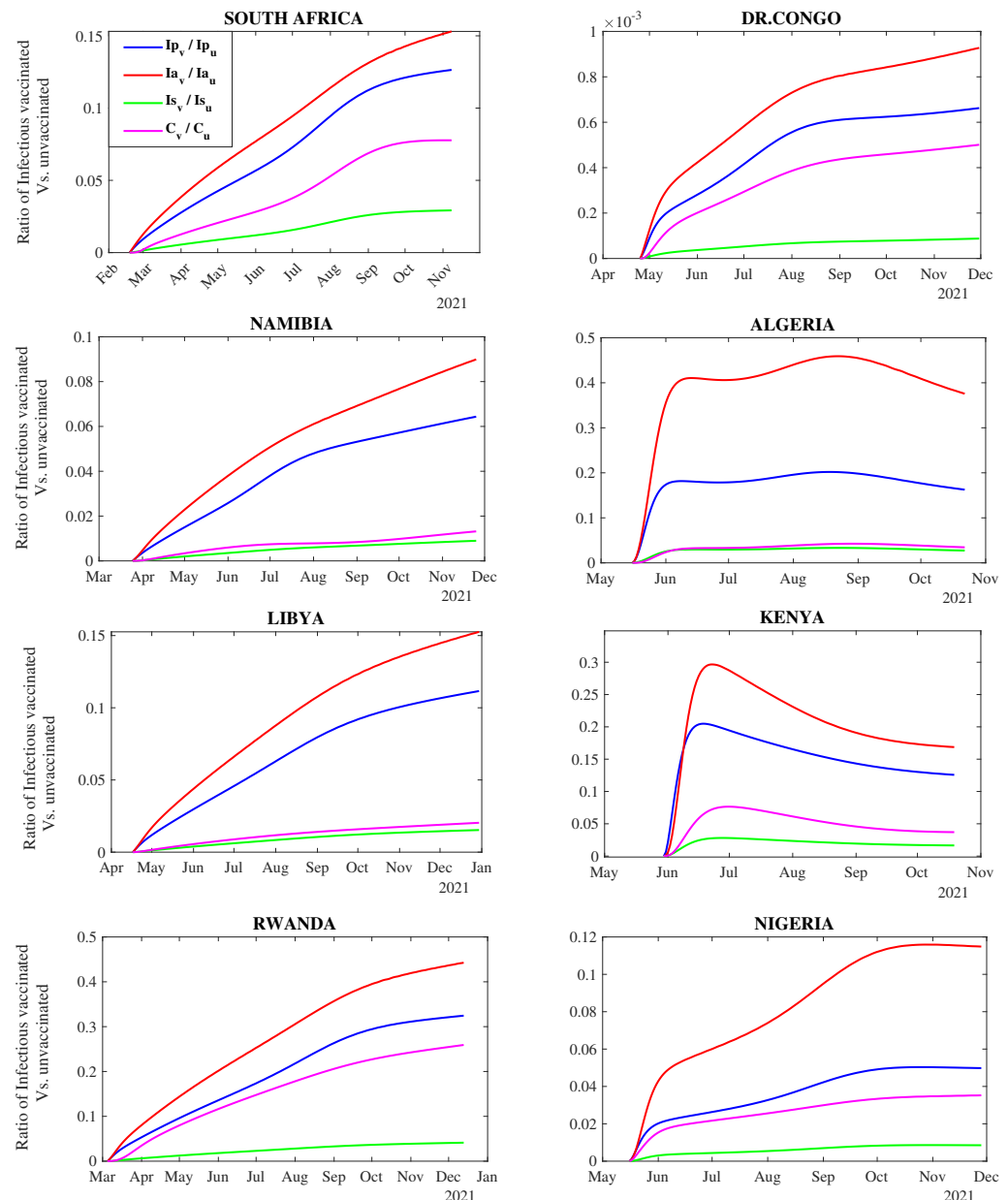

Figure 2. Evolution trend of each infectious compartment for vaccinated and unvaccinated individuals over time in each country. The first line (purple) in the legend depicts the ratio of the number of confirmed infectious vaccinated individuals to confirmed infectious unvaccinated individuals, the second line (green) depicts the ratio of the number of symptomatic infectious vaccinated individuals to the symptomatic infectious unvaccinated, the third line (red) depicts the ratio of the number of asymptomatic infectious vaccinated individuals to asymptomatic infectious unvaccinated, and the last line (blue) depicts the ratio of the number of pre-symptomatic infectious vaccinated individuals to pre-symptomatic infectious unvaccinated.

3.2.2. Impact of Vaccination on the Control Reproduction Number per Country

We computed the values for the control reproduction number, R_c using the fixed and estimated model parameters. Overall, the estimates for the R_c for the eight African countries during the third wave of the epidemic ranged from 1.911 (for Kenya) to 1.432 (for Libya), with an average of $R_c = 1.693$ (Table A7). Similarly, in the absence of vaccination and other control measures, we computed the values for the basic reproduction numbers, R_0, for each of the eight countries considered. The results indicated that overall, the values for these countries for R_0 are approximately two times higher than those for R_c. With an average of $R_0 = 2.843$, estimates for the R_0 were lowest for DR Congo (2.408) and highest for Algeria (3.640).

3.2.3. Impact of Vaccination on the Transmission Dynamics

We simulated the model to assess the impact of vaccination on the transmission dynamics of COVID-19 in each of the selected eight countries. Results from the simulation (Figure A2) suggest that vaccinated individuals had a much lower force of infection (the rate at which the susceptible individuals become infected per unit time or mass-action transmission) of COVID-19 and a reduced capacity for virus transmission. The reduction in the transmission rate (per capita rate at which two different individuals come in effective contact per unit time) due to vaccination was higher for countries such as Algeria, DR Congo, and Nigeria. However, in Kenya, the force of infection for vaccinated and unvaccinated individuals varies similarly over time.

In addition, we also estimated the infection probabilities and the relative infectiousness to describe the transmission dynamics of vaccinated and unvaccinated populations. The results in (Figure A3) show that the infection probability of disease transmission among the vaccinated population is lower than that among the unvaccinated. Furthermore, the infection probability of disease transmission from infectious unvaccinated to susceptible vaccinated is higher than that from infectious vaccinated to susceptible unvaccinated. The results from Figure A4 also revealed that the pre-symptomatic and asymptomatic vaccinated are less infectious than the vaccinated. However, both the vaccinated and unvaccinated are symptomatic and confirmed to be highly infectious.

3.2.4. Impact of Vaccination on COVID-19 Incidence among the Vaccinated and Unvaccinated Individuals

The vaccine effectiveness (expressed as a detection rate ratio) in reducing new infections for the pre-symptomatic, asymptomatic, and symptomatic cases for the vaccinated as compared to the unvaccinated across the considered African countries are presented in Figures 3a–c. The results from Figure 3 indicate higher heterogeneity in the vaccine efficacy (measured in terms of the detection rate ratio) among the asymptomatic cases compared to the pre-symptomatic and symptomatic cases. The results also showed that higher values for vaccine efficacy against new infections were reported among symptomatic cases (ranging from 0.3 to 5.22) as compared to the asymptomatic (0.118–1.0247) and pre-symptomatic (0.0492–0.89087) cases, indicating lower vaccine efficacy against new symptomatic cases.

The vaccine efficacy against new pre-symptomatic cases was generally less than one across the considered countries. With an expectation of Nigeria, the rest of the countries had detection rate ratio values less than 0.5. In Nigeria, the detection rate of COVID-19 infections among the pre-symptomatic vaccinated was about four times higher than that for the unvaccinated pre-symptomatic cases.

Similarly, the vaccine efficacy against new asymptomatic cases is relatively high (>0.5) for the majority of the considered African countries, as shown in Figure 3b. In DR Congo, there is no significant difference in the detection rates for new infections among vaccinated and unvaccinated individuals. On the other hand, in Algeria, the detection rate among the vaccinated was about 88.2% lower among the vaccinated as compared to the unvaccinated. Results further indicated that countries such as Namibia, South Africa, Libya, and Rwanda

had a similar detection rate ratio, implying that vaccinated individuals were at about 25% lower risk of becoming COVID-19 cases compared to the unvaccinated.

The results in Figure 3c also presented the vaccine efficacy against symptomatic cases across the considered African countries. The results indicate that countries with relatively high vaccine coverage, for instance, Rwanda, Kenya, and Algeria, had values for the detection rate ratio greater than one. For instance, in Rwanda, vaccinated people appear to be more than 5-fold to test positive for COVID-19 compared to unvaccinated people. However, in Kenya, since the detection rate ratio is approximately one, vaccinated and unvaccinated individuals are likely to have the same detection rate. On the other hand, in Namibia, the detection rate for the vaccinated symptomatic cases is 65% lower than that for the unvaccinated.
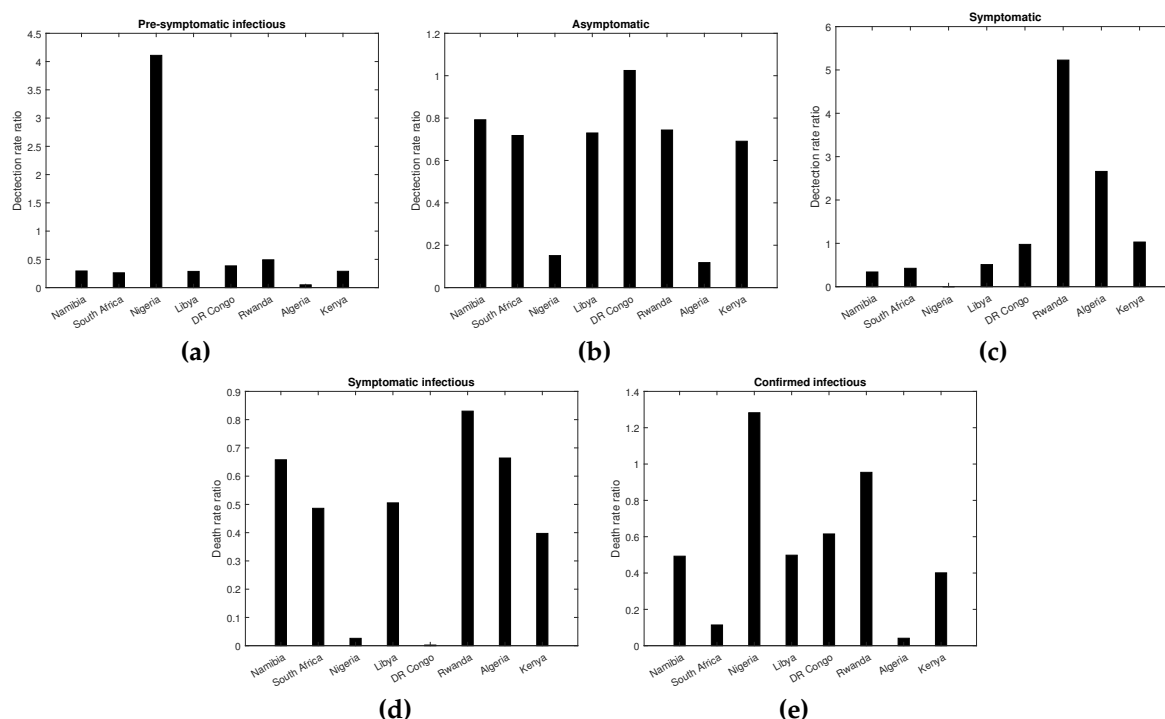

Figure 3. Vaccine effectiveness against COVID-19 infections and deaths. Panels (**a**–**c**) depict vaccine effectiveness against pre-symptomatic, asymptomatic, and symptomatic new infections Panels (**d**,**e**) present vaccine effectiveness against symptomatic and confirmed deaths.

3.2.5. Impact of Vaccination on COVID-19 Mortality among the Vaccinated and Unvaccinated Individuals

The impact of the vaccination on COVID mortality was quantified by the death rate ratio of the vaccinated compared to the unvaccinated for symptomatic and confirmed cases. The results are presented in Figure 3d,e. Our findings indicated a high variation in the vaccine efficacy against COVID-19 deaths among symptomatic and confirmed cases across the considered countries. Overall, vaccination had a higher impact in reducing COVID-19 deaths from confirmed cases compared to those from symptomatic cases, as shown by the lower values of the detection rate ratio for the confirmed. High vaccine efficacy against symptomatic COVID-19 deaths was recorded in the DR Congo (0.0023) and lowest in Rwanda (0.83) and Algeria (0.664). For instance, in DR Congo, the risk of COVID-19 among the symptomatic individuals is 99.76% lower among vaccinated individuals than the unvaccinated. For the confirmed cases, except for DR Congo and Rwanda, the vaccine efficacy against COVID-19 deaths is less than 0.5. A high vaccine efficacy against COVID-19-related deaths from confirmed cases was recorded in Algeria (0.041), South Africa (0.114) and Nigeria (0.132), while low vaccine efficacy was recorded in Rwanda (0.954).

3.2.6. Impact of Vaccine Coverage with Different Levels of Reduction in the Transmission Rate due to NPIs (ψ) among Unvaccinated and Vaccinated Individuals

Figure 4 shows the variation of R_c with respect to the vaccine coverage and different levels of reduction in the transmission rate due to adherence to non-pharmaceutical interventions (NPIs) among both vaccinated and unvaccinated individuals for each country. The results obtained, depicted in Figure 4, show that overall, in each of the considered countries, there is a decrease in the values of R_c with increasing vaccine coverage combined with a high reduction in the transmission rate due to NPIs by both vaccinated and unvaccinated individuals. The results showed that on average, at least 60% of each African country's population should be vaccinated to curtail the COVID-19 pandemic (lower the R_c below one). Moreover, lower values of R_c are possible even when there is a low or moderate reduction in the transmission rate due to NPIs.
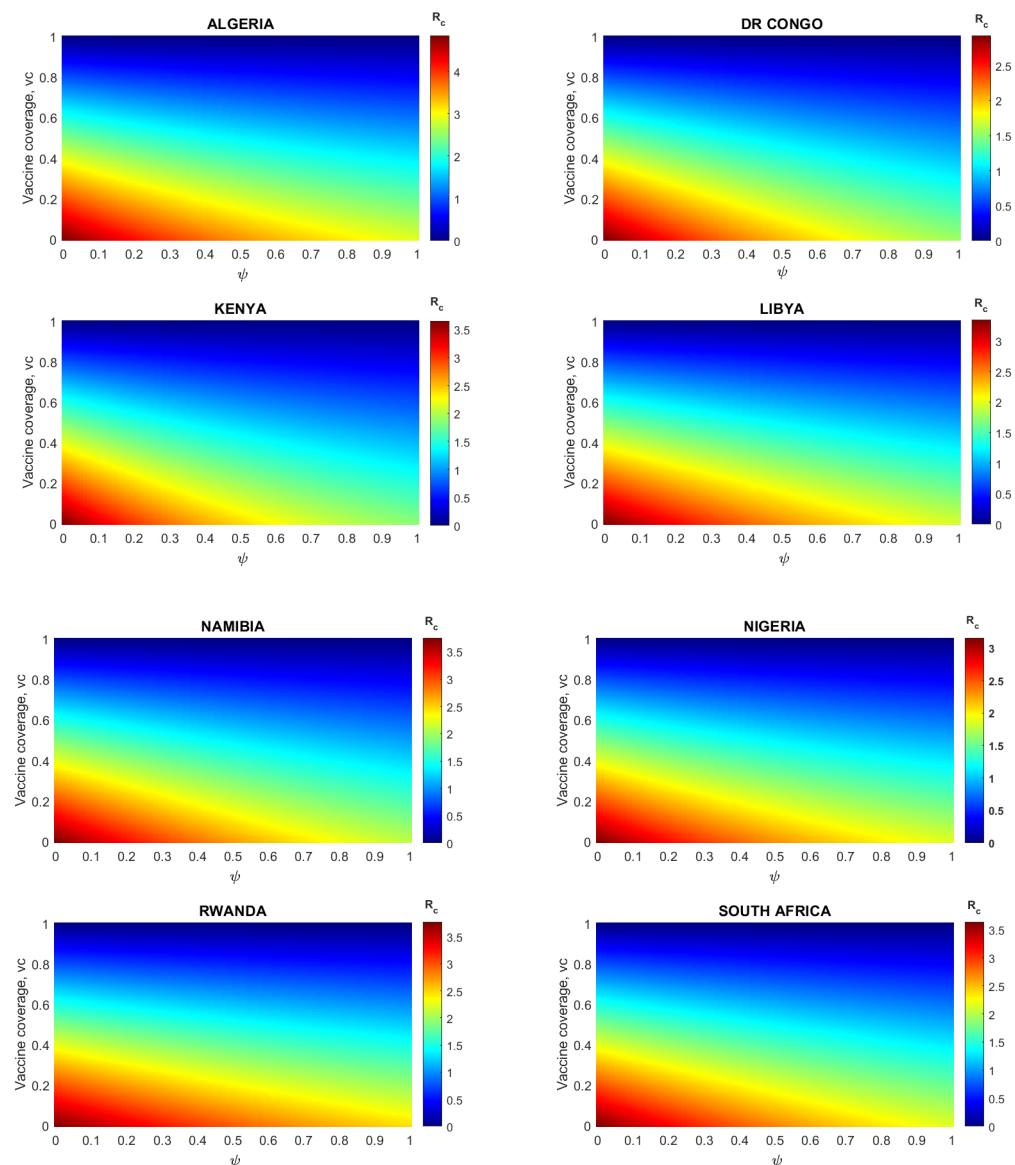

Figure 4. Contour plots of the control reproduction number (R_c) as functions of the vaccine coverage for different levels of reduction in the SARS-CoV-2 transmission rate due to control measures (ψ) among the unvaccinated and vaccinated individuals.

For instance, in Algeria, the minimum vaccine coverage required for $R_c < 1$ is 80%, assuming that there is no reduction in the transmission rate due to NPIs in vaccinated and unvaccinated populations (i.e., $\psi = 0$). However, when the reduction in the transmission rate due to NPIs among the unvaccinated and vaccinated individuals is increased to 10% (low) and 30% (moderate) during the vaccination period, the minimum vaccine coverage required to bring R_c to one is reduced to 75% and 70%, respectively.

In DR Congo, findings indicated that at least 65% of the unvaccinated population should be vaccinated for $R_c < 1$. In addition, the pandemic is curtailed when a 10%, 30%, and 50% reduction in the transmission rate due to NPIs is associated with 58%, 54%, and 50% vaccine coverage. The results further indicated that in most of the countries considered, vaccinating less than 50% (i.e., $VC > 50\%$) requires a high reduction in the transmission rate due to NPIs to contain the pandemic. For instance, in Kenya, when the proportion of unvaccinated individuals is below 50%, the $R_c > 1.5$. To reduce $R_c < 1$, a high reduction in the transmission rate due to NPIs is required (i.e., $\psi > 0.75$).

4. Discussion

In this study, we developed a mathematical model to assess the impact of vaccination programs on curtailing the burden of COVID-19 in eight selected African countries. The model stratifies the total population into two subgroups according to vaccination status. The model is fitted to cumulative daily case data for each selected country corresponding to the third wave of the pandemic. The unknown parameters are estimated using the nonlinear least square method. Overall, the model fits well with the actual cumulative number of confirmed cases for the selected countries.

Our results show the effectiveness of the COVID-19 vaccine against transmission of the SARS-CoV-2 virus to the susceptible contacts from infected vaccinated cases, which is shown by the lower infection probabilities among the vaccinated individuals. These findings are consistent with a study by As et al. [41] that showed a substantial reduction in the transmission risk of PCR-confirmed SARS-CoV-2 infection among vaccinated healthcare workers. Most studies have shown viral load to be an important indicator of the relative infectiousness of both vaccinated and unvaccinated individuals [42]. Our findings suggest that the relative infectiousness of the vaccinated asymptomatic infectious individuals is lower than that of the symptomatic infectious individuals. For example, in South Africa, asymptomatic vaccinated individuals were about three times more infectious than pre-symptomatic. This would be because the asymptomatic individuals shed the virus faster than the pre-symptomatic and symptomatic cases, implying a shorter infectious period [43].

According to the study by Chen et al. [44], asymptomatic cases of COVID-19 are a potential source of substantial spread of the disease, accounting for two-thirds of COVID-19 infections in Africa. Our study findings support this hypothesis, which is indicated by the increased number of both vaccinated and unvaccinated asymptomatic and pre-symptomatic individuals over time. The high proportion of infected individuals without symptoms will likely lead to an under-representation of the number of infections reported in African countries. Therefore, in addition to vaccination, strategies such as mass testing and testing of the asymptomatic close contacts should be implemented to control SARS-CoV-2 transmission in African countries. On the other hand, vaccination programs significantly reduced the number of symptomatic individuals.

The results show that the average control reproduction number across the eight African countries during the first months of vaccination is 1.693, which is greater than one. This suggests that each infectious individual can transmit COVID-19 to two people. The epidemiological implication is that COVID-19 will continue to spread in most African countries even after vaccination but at a slower rate than in the absence of a vaccine. Our findings show that the vaccine's effectiveness in reducing the detection of new infections is higher among the asymptomatic and pre-symptomatic cases than the symptomatic cases. For instance, in Rwanda, the vaccinated symptomatic individuals are 5-fold more likely to test positive for COVID-19 than the unvaccinated individuals. This implies low vaccine

efficacy against new symptomatic infections. This is evidenced by the high detection rates for the symptomatic individuals ranging from 0% to 0.86%. This may be partly due to the low efficacy of the vaccines currently administered to people in many African countries. These findings align with the vaccine impact on new COVID-19 infections reported in clinical trials [45,46].

Vaccination also had a significant impact in reducing COVID-19 deaths that arise from confirmed cases as compared to symptomatic cases. We also observed high variation in the vaccine effectiveness against COVID-19 deaths across all the considered countries. This would be due to different levels of vaccine coverage, economic levels, control measures, testing, and reporting efforts [47]. Furthermore, we observed that countries with high vaccination coverage, such as South Africa and Algeria, had a greater reduction in the mortality rates for confirmed cases compared to largely unvaccinated countries.

Numerical sensitivity analysis performed to evaluate the combined impact of vaccination with different levels of adherence to NPIs showed that to eradicate the pandemic, at least 60% of the population in each African country should be vaccinated, combined with low to high NPI adherence by unvaccinated and vaccinated individuals. Our findings align with the African Centres for Disease Control's COVID-19 program [48] recommendation that 70% of the population should be fully vaccinated. It should be noted that achieving herd immunity is vital, particularly in the African continent, which is mostly dominated by a large proportion of young people and given the low vaccine supply. However, despite this recommendation and the results of our model, it may take longer for most African countries to reach herd immunity, given the current low vaccine coverage levels in Africa. In addition to the low supply of COVID-19 vaccines [49], many Africans are also unwilling to be vaccinated, as many African countries, for instance, DR Congo, still have thousands to millions of doses that are yet to be administered.

This study has some limitations. We modeled vaccine effectiveness against transmission, new COVID-19 infections, and deaths. However, these estimates may vary according to the significant difference between men and women in the death rate for COVID-19, age structure of the population, specific COVID-19 variants in each country, and multiple COVID-19 vaccine doses administered. In addition, the proposed modeling framework can be extended to include data for all the waves of the pandemic, not just the third wave. Furthermore, the study considered a constant vaccination rate which may not be realistic, as the vaccination rate may depend on the number of vaccine doses available on a particular day. Hence, considering the time-dependent vaccination rate may improve the accuracy of the VE estimates.

5. Conclusions

Vaccination programs significantly reduce the transmission as well as relative infectiousness among vaccinated individuals. COVID-19 vaccines prevent COVID-19 disease by reducing the probability of developing symptoms. The study also pointed out that a large proportion of the undetected cases are pre-symptomatic and asymptomatic. This may increase the rate at which susceptible individuals acquire infection, since such individuals are unaware they are sick and are less likely to adhere to NPIs. This study showed that the likelihood of achieving vaccine-derived herd immunity in most African countries is very promising, especially if the vaccination program is complemented with low or moderate levels of adherence to NPIs among both vaccinated and unvaccinated individuals. These results may vary according to the significant difference between men and women in the death rate for COVID-19, the age structure of the population, specific COVID-19 variants in each country, and multiple COVID-19 vaccine doses administered. However, achieving herd immunity in Africa is largely hindered by widespread vaccine hesitancy. It is therefore important for the African governments to design vaccination strategies that address vaccine hesitancy, such as an incentive-based approach, where individuals are given incentives such as food items, beverages, snacks, and T-shirts at the points of vaccination. This may yield positive results for mass vaccination as it will encourage more people to get vaccinated,

thus giving indirect protection against the disease to individuals who cannot get vaccinated, such as children, and pregnant women, thus achieving herd immunity.

Author Contributions: Conceptualization, R.G.K. and R.N.; methodology, R.G.K., R.N. and Y.M.; software, R.N., R.G.K. and Y.M.; validation, J.T.D. and R.G.K.; formal analysis, R.N., Y.M. and P.A.; data curation, R.N. and P.A.; writing—original draft preparation, R.N.; writing—review and editing, Y.M., R.N., P.A., J.T.D., B.E.L., V.K.S., M.W. and R.G.K.; supervision, R.G.K. All authors have read and agreed to the published version of the manuscript.

Data Availability Statement: All the data used are provided within the manuscript.

Conflicts of Interest: The authors declare no conflict of interest.

Appendix A

Table A1. Selected countries in each region with their start date and end date.

Selected Countries	Start Date	End Date
DR Congo	25 April 2021	30 November 2021
Rwanda	5 March 2021	13 December 2021
Kenya	30 May 2021	19 October 2021
Algeria	4 January 2021	29 October 2021
Libya	13 January 2021	13 December 2021
Namibia	25 March 2021	25 November 2021
South Africa	18 February 2021	8 November 2021
Nigeria	16 May 2021	28 November 2021

Table A2. Fixed model parameters, their description and value.

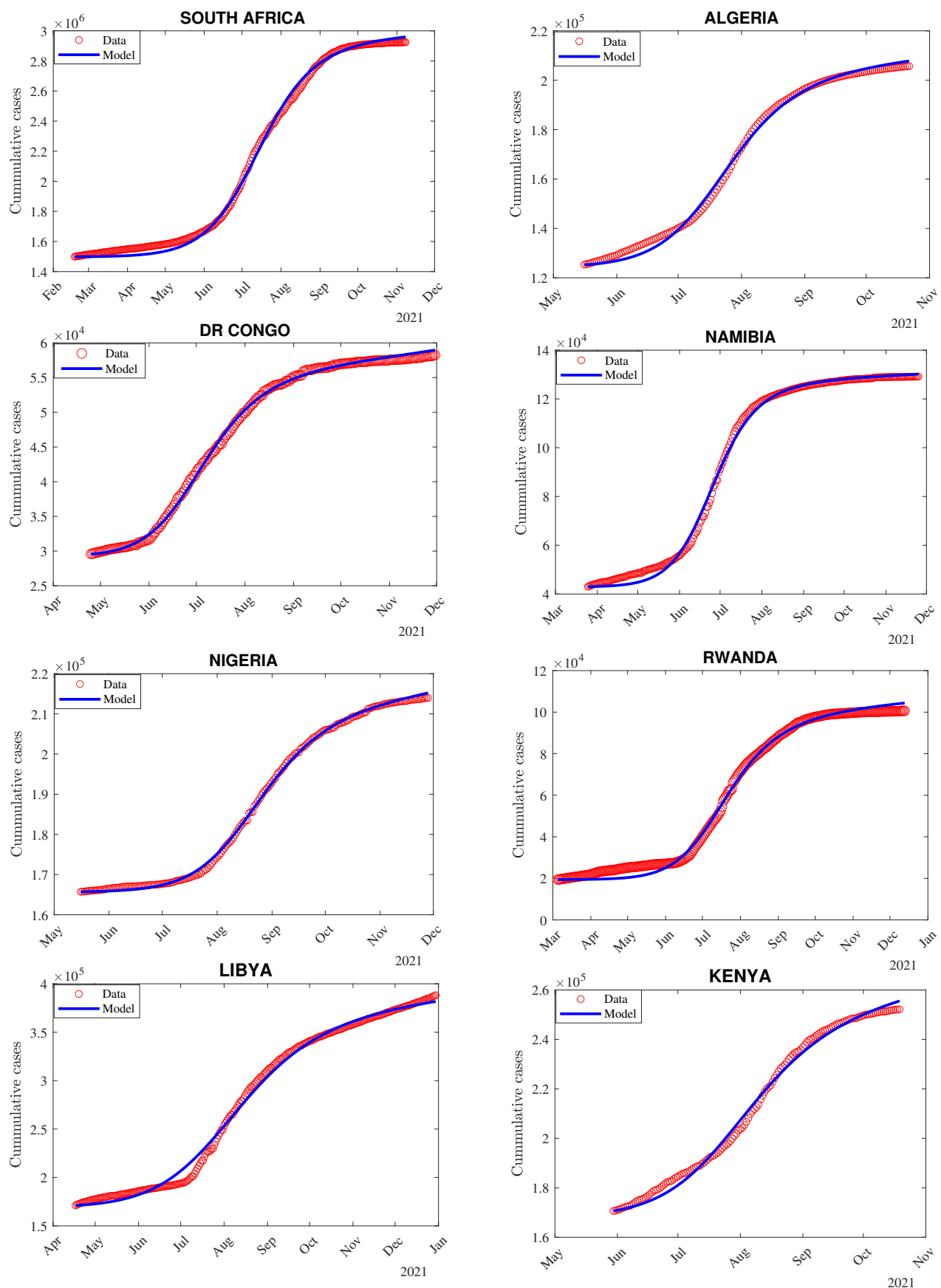| Parameter	Value	References
d_u	1/270 day $^{-1}$	[50]
d_v	1/270 day $^{-1}$	[51]
ω	1/180 day $^{-1}$	[52]
α_E	3.3 days	[53]
α_p	3.2 days	[25]
ρ_1	0.6	[54]
ρ_2	0.1	[55]
γ_{a_1}	1/5 day $^{-1}$	[29,54]
γ_{a_2}	1/3.4 day $^{-1}$	[29,54]
γ_{s_1}	1/10 day $^{-1}$	[29,54]
γ_{s_2}	1/8 day $^{-1}$	[29,54]
γ_{c_1}	1/11 day $^{-1}$	[29,54]
γ_{c_2}	1/10 day $^{-1}$	[29,54]

Figure A1. Plots depicting the fitting of the model to the cumulative confirmed COVID-19 cases for selected African countries.
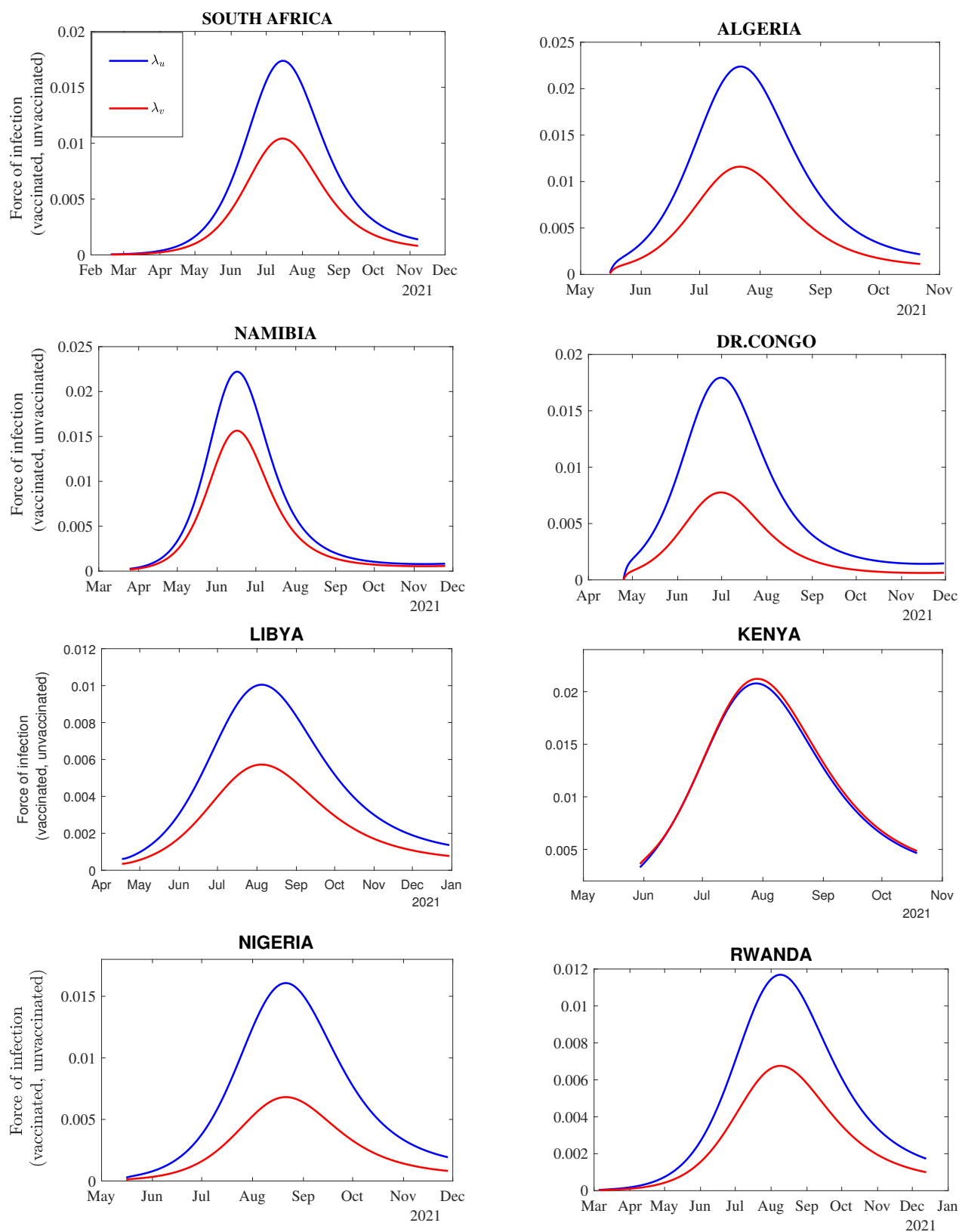
Figure A2. Dynamic trend for the force of infection over time during COVID-19 vaccination. The blue and red curves represent the force of infection for the unvaccinated (λ_u) and vaccinated (λ_v) individuals, respectively.
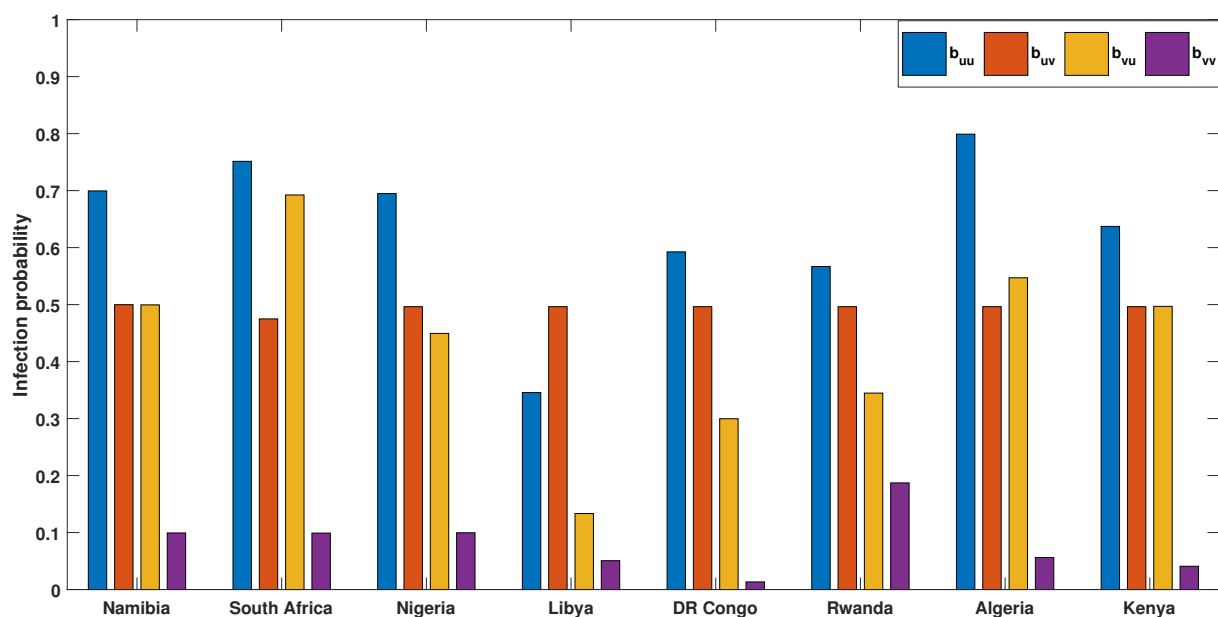
Figure A3. Bar plot presenting the estimated infection probabilities for vaccinated and unvaccinated individuals for selected African countries.

Figure A4. Plots presenting the estimated relative infectiousness for vaccinated and unvaccinated individuals for selected African countries. (**A**) Pre-symptomatic infectious, (**B**) Asymptomatic infectious, (**C**) Symptomatic infectious, and (**D**) Confirmed infectious.

Table A3. Fixed parameters, their values and sources varying per country.

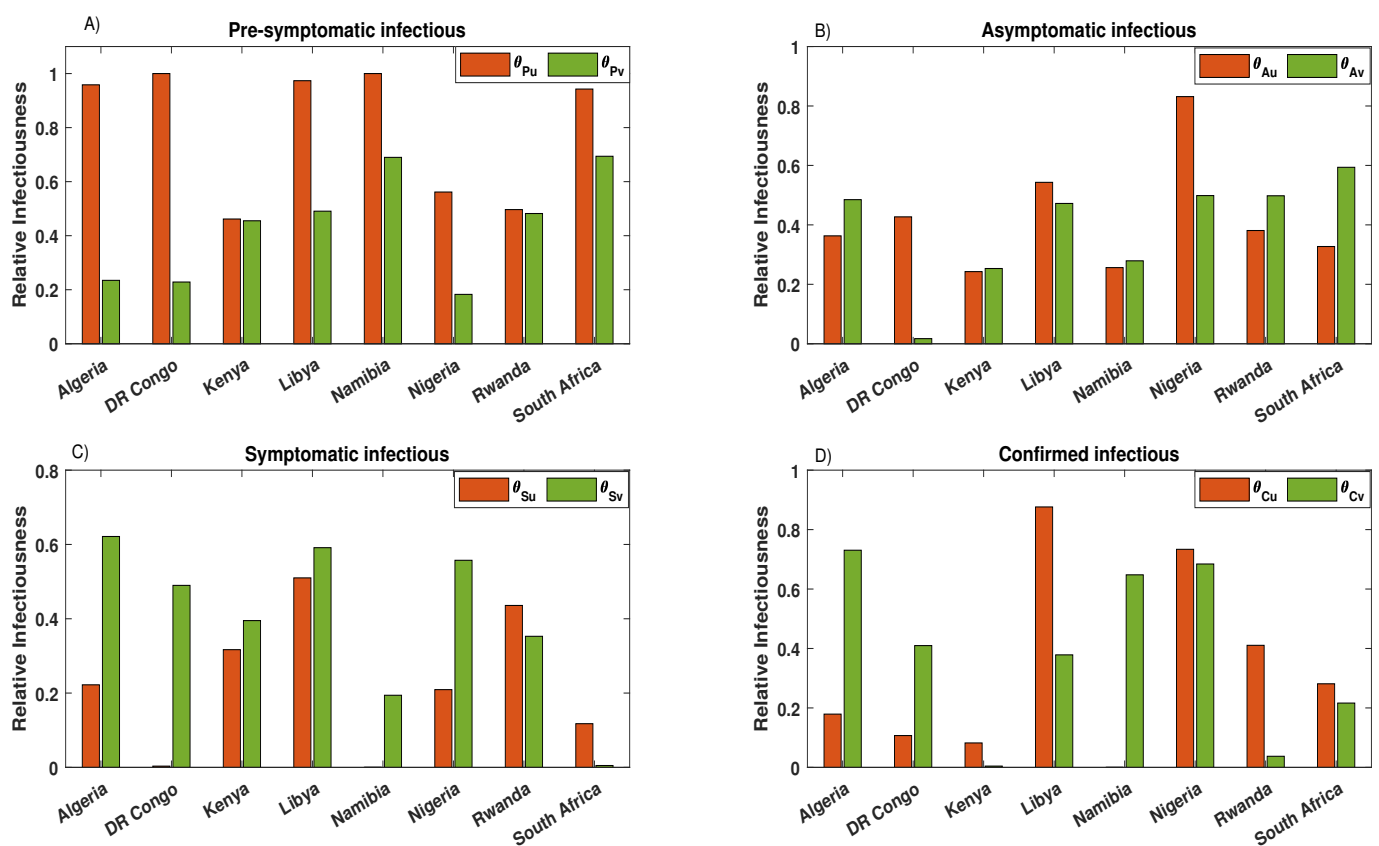| Parameters	Countries							
	Algeria	**DR Congo**	**Kenya**	**Libya**	**Namibia**	**Nigeria**	**Rwanda**	**South Africa**
L.E	77.5	61.6	67.5	73.4	64.9	55.8	70.0	64.9
N_0	44,177,969	95,894,118	53,005,614	6,735,277	2,530,151	213,401,323	13,461,888	59,392,255
μ	3.5×10^{-5}	4.4×10^{-5}	4×10^{-5}	3.7×10^{-5}	4.2×10^{-5}	4.9×10^{-5}	3.9×10^{-5}	4.2×10^{-5}
Λ	6227.61	17,591.26	10,285.07	433.56	264.94	39,787.80	1424.71	4999.12
VC	13.62%	0.15%	6.38%	27.5%	13.69%	3.00%	35.5%	26.6%
VP	160	220	143	258	246	197	284	264
ν	0.00085	0.00001	0.00045	0.00107	0.00056	0.00015	0.00125	0.00101
ψ_1	0.35	0.30	0.15	0.35	0.30	0.45	0.45	0.45
ψ_2	0.25	0.25	0.18	0.25	0.25	0.25	0.25	0.45

Table A4. Values for the Initial conditions for the state variables and 95%CI.

Country	$S_{u0}\,(\times 10^6)$	E_{u0}	I_{pu0}	I_{Au0}	I_{Su0}	R_{u0}
Namibia	1.66 [1.57, 1.74]	1500.00 [1365.29, 1634.70]	700.15 [641.35, 758.9]	706.06 [675.15, 736.97]	700.00 [672.02, 727.97]	144.62 [105.10, 184.14]
South Africa	44.87 [43.13, 46.60]	4763.61 [4179.73, 5347.49]	5499.92 [5214.45, 5785.39]	1322.84 [970.52, 1675.16]	265.16 [223.47, 306.86]	455.28 [416.41, 494.15]
Nigeria	49.94 [30.06, 69.72]	76,207.26 [72,089.64, 80,324.87]	39,377.52 [36,424.84, 242,330.20]	12,989.71 [11,127.50, 14,851.92]	571.77 [425.02, 718.52]	346.74 [194.97, 498.51]
Libya	4.19 [3.80, 4.58]	10043.62 [9799.05, 10,288.17]	7097.94 [6808.63, 7387.25]	5144.00 [4593.28, 5694.72]	2500.26 [2252.15, 2748.37]	1159.89 [1058.219, 1261.57]
DR.Congo	7.14 [2.09, 12.19]	69,889.75 [66,287.98, 73,491.51]	1002.16 [902.45, 1101.87]	541.19 [442.15, 640.22]	784.58 [734.78, 834.37]	249.44 [230.28, 268.59]
Rwanda	13.35 [12.58, 14.13]	3191.59 [2882.33, 3500.86]	1120.60 [1041.19, 1200.01]	1011.78 [858.52, 1165.04]	741.58 [714.24, 768.93]	251.03 [208.27, 293.79]
Algeria	9.58 [5.42, 13.72]	93,208.19 [88,602.33, 97,814.04]	4344.26 [3988.51, 4700.00]	530.67 [115.97, 945.38]	581.77 [542.56, 620.99]	100.51 [63.13, 137.89]
Kenya	4.32 [4.06, 4.55]	77,571.99 [68,155.25, 86,988.73]	44,589.27 [41,245.57, 47,932.96]	34,186.64 [31,497.56, 36,875.72]	13,641.08 [12,529.16, 14,753.01]	962.79 [924.76, 1000.82]

Table A5. Estimated (fitted) parameter values and their 95% CI for the model for each selected country.

Parameter	Namibia	South Africa	Nigeria	Libya
b_{uu}	0.69943 [0.66876, 0.73010]	0.75138 [0.70816, 0.79461]	0.68895 [0.64075, 0.73716]	0.34566 [0.31123, 0.38009]
b_{uv}	0.49986 [0.46100, 0.53872]	0.47487 [0.43008, 0.51967]	0.29131 [0.25009, 0.33253]	0.19777 [0.18971, 0.20583]
b_{vu}	0.49949 [0.44789, 0.55109]	0.69237 [0.62429, 0.76045]	0.20114 [0.14281, 0.25947]	0.13348 [0.11327, 0.15354]
b_{vv}	0.09929 [0.09199, 0.10658]	0.09903 [0.09701, 0.10105]	0.09582 [0.09138, 0.10026]	0.05061 [0.04610, 0.05513]
θ_{Pu}	0.99999 [0.90132, 1.09866]	0.94265 [0.85095, 1.03434]	0.81294 [0.69935, 0.92650]	0.97356 [0.88567, 1.06144]
θ_{Au}	0.25624 [0.17032, 0.34215]	0.32720 [0.24394, 0.41045]	0.32603 [0.22519, 0.42687]	0.54310 [0.44715, 0.63904]
θ_{Su}	0.00012 [−0.0679, 0.06822]	0.11758 [0.02434, 0.21083]	0.64576 [0.83210, 0.96535]	0.51002 [0.47033, 0.54970]
θ_{Cu}	0.01583 [−0.0229, 0.05461]	0.28121 [0.20859, 0.35382]	0.88343 [0.79233, 0.97452]	0.87620 [0.78317, 0.96922]
θ_{Pv}	0.68982 [0.61379, 0.76585]	0.69391 [0.61708, 0.77070]	0.89522 [0.77477, 1.01567]	0.49071 [0.44117, 0.52506]
θ_{Av}	0.27906 [0.20984, 0.34828]	0.59369 [0.52832, 0.65905]	0.91138 [0.79100, 1.03177]	0.47209 [0.42120, 0.52289]
θ_{Sv}	0.19411 [0.12131, 0.26691]	0.00502 [-0.0760, 0.08605]	0.85105 [0.75183, 0.95027]	0.59134 [0.52606, 0.65661]
θ_{Cv}	0.64782 [0.57741, 0.71824]	0.21637 [0.13351, 0.29921]	0.63620 [0.56903, 0.70337]	0.37854 [0.32847, 0.42861]
q_{p1}	0.00499 [0.00492, 0.00506]	0.00499 [0.00496, 0.00502]	0.00006 [−0.0002, 0.00019]	0.00486 [0.00440, 0.00532]
q_{p2}	0.00067 [0.00063, 0.00072]	0.00131 [0.00126, 0.00135]	0.00026 [0.00018, 0.00034]	0.00139 [0.00129, 0.00149]
q_{a1}	0.00498 [0.00465, 0.00532]	0.00497 [0.00489, 0.00505]	0.00027 [−0.00004, 0.0006]	0.00351 [0.00309, 0.00392]
q_{a2}	0.00395 [0.00371, 0.00419]	0.00256 [0.00253, 0.00265]	0.00004 [−0.0003, 0.00040]	0.00256 [0.00237, 0.00276]
q_{s1}	0.00868 [0.00824, 0.00913]	0.00839 [0.00829, 0.00851]	0.00031 [−0.0005, 0.00114]	0.00862 [0.00792, 0.00933]
q_{s2}	0.00294 [0.00280, 0.00309]	0.00356 [0.00341, 0.00372]	0.000004 [−0.0004, 0.0004]	0.00439 [0.00407, 0.00472]
δ_{s1}	0.00029 [0.00028, 0.00031]	0.19703 [0.17974, 0.00211]	0.00567 [0.00458, 0.00677]	0.00197 [0.00183, 0.02114]
δ_{s2}	0.00019 [0.00018, 0.00020]	0.09581 [0.08846, 0.10316]	0.00015 [−0.0007, 0.00098]	0.00099 [0.00182, 0.00217]
δ_{c1}	0.00040 [0.00038, 0.00042]	0.19959 [0.17916, 0.22004]	0.00298 [0.00221, 0.00375]	0.00199 [0.01899, 0.02094]
δ_{c2}	0.00019 [0.00018, 0.00020]	0.02278 [0.01553, 0.03003]	0.00382 [0.00308, 0.00457]	0.00099 [0.00090, 0.00108]

Table A6. Estimated parameter values and their 95% CI for the model for each selected country.

Parameter	Rwanda	Algeria	Kenya	DR Congo
b_{uu}	0.56684 [0.54223, 0.59140]	0.79907 [0.74159, 0.85655]	0.63721 [0.58228, 0.69215]	0.59252 [0.55302, 0.63202]
b_{uv}	0.32961 [0.28843, 0.37078]	0.44401 [0.39858, 0.48943]	0.69956 [0.66150, 0.73763]	0.25625 [0.18964, 0.32285]
b_{vu}	0.34471 [0.30639, 0.38305]	0.54705 [0.48178, 0.61232]	0.49691 [0.46349, 0.53033]	0.29970 [0.26933, 0.33008]
b_{vv}	0.18714 [0.17146, 0.20282]	0.05621 [0.05062, 0.06181]	0.04087 [0.02406, 0.05769]	0.01336 [0.00516, 0.02154]
θ_{Pu}	0.49657 [0.45476, 0.53838]	0.95831 [0.90050, 1.01612]	0.46168 [0.42345, 0.49992]	0.99997 [0.94617, 1.05378]
θ_{Au}	0.38102 [0.32949, 0.43255]	0.36306 [0.26965, 0.45647]	0.24275 [0.21254, 0.27297]	0.42697 [0.33455, 0.51938]
θ_{Su}	0.43582 [0.41439, 0.45727]	0.22221 [0.11050, 0.33392]	0.31683 [0.26989, 0.36376]	0.00335 [−0.0765, 0.08316]
θ_{Cu}	0.41064 [0.35984, 0.46145]	0.17918 [0.09015, 0.26821]	0.08219 [0.03981, 0.12458]	0.10705 [0.05563, 0.15847]
θ_{Pv}	0.48203 [0.43416, 0.52992]	0.23469 [0.15878, 0.31059]	0.45516 [0.41124, 0.49907]	0.22848 [0.17245, 0.28450]
θ_{Av}	0.49791 [0.44987, 0.54594]	0.48487 [0.42802, 0.54172]	0.25320 [0.23014, 0.27626]	0.01724 [−0.0390, 0.07350]
θ_{Sv}	0.35278 [0.31528, 0.39029]	0.62145 [0.55725, 0.68564]	0.39507 [0.35426, 0.43587]	0.48985 [0.44160, 0.5380]
θ_{Cv}	0.03734 [0.00201, 0.07265]	0.73060 [0.65886, 0.80235]	0.00433 [−0.0367, 0.04540]	0.40973 [0.35467, 0.4648]
q_{p1}	0.00019 [0.00018, 0.00022]	0.00163 [0.00109, 0.00215]	0.00019 [0.00018, 0.00021]	0.00073 [0.00053, 0.00092]
q_{p2}	0.00010 [0.00009, 0.00011]	0.00008 [0.00007, 0.00009]	0.00006 [0.00005, 0.00010]	0.00028 [0.00020, 0.00035]
q_{a1}	0.00254 [0.00227, 0.00281]	0.00025 [−0.0003, 0.00079]	0.00288 [0.00269, 0.00306]	0.00095 [0.00077, 0.00113]
q_{a2}	0.00189 [0.00170, 0.00208]	0.00003 [−0.0002, 0.00026]	0.00199 [0.00185, 0.00213]	0.00097 [0.00089, 0.00106]
q_{s1}	0.00018 [−0.0003, 0.00064]	0.00130 [0.00042, 0.00218]	0.00192 [0.00171, 0.00213]	0.000009 [−0.0004, 0.0005]
q_{s2}	0.00091 [0.00086, 0.00096]	0.003461 [0.0031, 0.00387]	0.00198 [0.00180, 0.00216]	0.00001 [0.00000, 0.00002]
δ_{s1}	0.00023 [0.00020, 0.00025]	0.00025 [0.00022, 0.00027]	0.00029 [0.00027, 0.00032]	0.00026 [0.00023, 0.00028]
δ_{s2}	0.00019 [0.00018, 0.00020]	0.00017 [0.00012, 0.00021]	0.00012 [0.00010, 0.00013]	0.000001 [0.0000, 0.00002]
δ_{c1}	0.00021 [0.00019, 0.00023]	0.00052 [0.00048, 0.00056]	0.00014 [0.00013, 0.00015]	0.00029 [0.00028, 0.00031]
δ_{c2}	0.00019 [0.00019, 0.00021]	0.00002 [−0.00001, 0.00005]	0.00006 [0.00005, 0.00010]	0.00018 [0.00016, 0.00020]

Table A7. Estimated values for the basic and control reproduction numbers and its components for each country with 95% confidence interval.

Parameter	R_{c1}	R_{c2}	R_{c3}	R_c	R_0
Namibia	0.813 [0.775, 0.851]	0.011 [0.009, 0.013]	0.889 [0.851, 0.927]	**1.713 [1.639, 1.788]**	**2.569 [2.449, 2.688]**
South Africa	0.670 [0.658, 0.683]	0.002 [0.015, 0.017]	0.800 [0.786, 0.820]	**1.500 [1.464, 1.515]**	**3.131 [3.099, 3.163]**
Nigeria	0.777 [0.749, 0.829]	0.021 [0.019, 0.024]	0.801 [0.772, 0.829]	**1.599 [1.554, 1.643]**	**3.157 [3.049, 3.265]**
Libya	0.699 [0.682, 0.716]	0.010 [0.009, 0.012]	0.723 [0.707, 0.739]	**1.432 [1.399, 1.464]**	**2.586 [2.525, 2.647]**
DR Congo	0.841 [0.778, 0.903]	0.00 [0.000, 0.001]	0.841 [0.778, 0.903]	**1.682 [1.557, 1.808]**	**2.407 [2.228, 2.587]**
Rwanda	0.853 [0.841, 0.865]	0.040 [0.036, 0.044]	0.912 [0.896, 0.928]	**1.806 [1.781, 1.831]**	**2.817 [2.777, 2.856]**
Algeria	0.908 [0.805, 1.011]	0.007 [0.005, 0.009]	0.987 [0.8797, 1.094]	**1.902 [1.026, 2.237]**	**3.640 [2.893, 3.634]**
Kenya	0.225 [0.222, 0.227]	0.836 [0.801, 0.872]	0.007 [0.004, 0.011]	**1.911 [1.864, 1.986]**	**2.438 [2.335, 2.543]**

References

1. Niu, Y.; Rui, J.; Wang, Q.; Zhang, W.; Chen, Z.; Xie, F.; Zhao, Z.; Lin, S.; Zhu, Y.; Wang, Y.; et al. Containing the transmission of COVID-19: A modeling study in 160 countries. *Front. Med.* **2021**, *8*, 701836. [CrossRef]
2. Khalifa, S.A.; Swilam, M.M.; El-Wahed, A.A.A.; Du, M.; El-Seedi, H.H.; Kai, G.; Masry, S.H.; Abdel-Daim, M.M.; Zou, X.; Halabi, M.F.; et al. Beyond the Pandemic: COVID-19 Pandemic Changed the Face of Life. *Int. J. Environ. Res. Public Health* **2021**, *18*, 5645. [CrossRef] [PubMed]
3. Spiteri, G.; Fielding, J.; Diercke, M.; Campese, C.; Enouf, V.; Gaymard, A.; Bella, A.; Sognamiglio, P.; Moros, M.J.S.; Riutort, A.N.; et al. First cases of coronavirus disease 2019 (COVID-19) in the WHO European Region, 24 January to 21 February 2020. *Eurosurveillance* **2020**, *25*, 2000178. [CrossRef] [PubMed]
4. Bouba, Y.; Tsinda, E.K.; Fonkou, M.D.M.; Mmbando, G.S.; Bragazzi, N.L.; Kong, J.D. The determinants of the low COVID-19 transmission and mortality rates in Africa: A cross-country analysis. *Front. Public Health* **2021**, *9*, 751197. [CrossRef]
5. WHO. *Weekly Bulletin on Outbreak and other Emergencies: Week 12: 14–20 March 2022*; Technical documents; World Health Organization. Regional Office for Africa: Brazzaville, Republic of Congo, 2022.
6. Mendez-Brito, A.; El Bcheraoui, C.; Pozo-Martin, F. Systematic review of empirical studies comparing the effectiveness of non-pharmaceutical interventions against COVID-19. *J. Infect.* **2021**, *83*, 281–293. [CrossRef] [PubMed]
7. Ejigu, B.A.; Asfaw, M.D.; Cavalerie, L.; Abebaw, T.; Nanyingi, M.; Baylis, M. Assessing the impact of non-pharmaceutical interventions (NPI) on the dynamics of COVID-19: A mathematical modelling study of the case of Ethiopia. *PLoS ONE* **2021**, *16*, e0259874. [CrossRef] [PubMed]

8. Cai, C.; Peng, Y.; Shen, E.; Huang, Q.; Chen, Y.; Liu, P.; Guo, C.; Feng, Z.; Gao, L.; Zhang, X.; et al. A comprehensive analysis of the efficacy and safety of COVID-19 vaccines. *Mol. Ther.* **2021**, *29*, 2794–2805. [CrossRef]
9. Ngonghala, C.N.; Iboi, E.; Eikenberry, S.; Scotch, M.; MacIntyre, C.R.; Bonds, M.H.; Gumel, A.B. Mathematical assessment of the impact of non-pharmaceutical interventions on curtailing the 2019 novel Coronavirus. *Math. Biosci.* **2020**, *325*, 108364. [CrossRef]
10. Wang, R.; Zhang, Q.; Ge, J.; Ren, W.; Zhang, R.; Lan, J.; Ju, B.; Su, B.; Yu, F.; Chen, P.; et al. Analysis of SARS-CoV-2 variant mutations reveals neutralization escape mechanisms and the ability to use ACE2 receptors from additional species. *Immunity* **2021**, *54*, 1611–1621. [CrossRef]
11. Shattock, A.J.; Le Rutte, E.A.; Dünner, R.P.; Sen, S.; Kelly, S.L.; Chitnis, N.; Penny, M.A. Impact of vaccination and non-pharmaceutical interventions on SARS-CoV-2 dynamics in Switzerland. *Epidemics* **2022**, *38*, 100535. [CrossRef]
12. Yang, B.; Yu, Z.; Cai, Y. The impact of vaccination on the spread of COVID-19: Studying by a mathematical model. *Phys. A Stat. Mech. Its Appl.* **2022**, *590*, 126717. [CrossRef]
13. Randolph, H.E.; Barreiro, L.B. Herd immunity: Understanding COVID-19. *Immunity* **2020**, *52*, 737–741. [CrossRef] [PubMed]
14. Knoll, M.D.; Wonodi, C. Oxford–AstraZeneca COVID-19 vaccine efficacy. *Lancet* **2021**, *397*, 72–74. [CrossRef] [PubMed]
15. Loembé, M.M.; Nkengasong, J.N. COVID-19 vaccine access in Africa: Global distribution, vaccine platforms, and challenges ahead. *Immunity* **2021**, *54*, 1353–1362. [CrossRef]
16. COVID-19 Vaccination Rate in Africa 2022, by Country. Available online: https://www.statista.com/statistics/1221298/covid-19 -vaccination-rate-in-african-countries. (accessed on 26 August 2022).
17. Nachega, J.B.; Sam-Agudu, N.A.; Masekela, R.; van der Zalm, M.M.; Nsanzimana, S.; Condo, J.; Ntoumi, F.; Rabie, H.; Kruger, M.; Wiysonge, C.S.; et al. Addressing challenges to rolling out COVID-19 vaccines in African countries. *Lancet Glob. Health* **2021**, *9*, e746–e748. [CrossRef] [PubMed]
18. Al-Kassim Hassan, M.; Adam Bala, A.; Jatau, A.I. Low rate of COVID-19 vaccination in Africa: A cause for concern. *Ther. Adv. Vaccines Immunother.* **2022**, *10*, 25151355221088159. [CrossRef] [PubMed]
19. Bernal, J.L.; Andrews, N.; Gower, C.; Gallagher, E.; Simmons, R.; Thelwall, S.; Stowe, J.; Tessier, E.; Groves, N.; Dabrera, G.; et al. Effectiveness of COVID-19 vaccines against the B. 1.617. 2 (Delta) variant. *N. Engl. J. Med.* **2021**, *385*, 585–594. [CrossRef]
20. Dagan, N.; Barda, N.; Kepten, E.; Miron, O.; Perchik, S.; Katz, M.A.; Hernán, M.A.; Lipsitch, M.; Reis, B.; Balicer, R.D. BNT162b2 mRNA COVID-19 vaccine in a nationwide mass vaccination setting. *N. Engl. J. Med.* **2021**, *384*, 1412-1423. [CrossRef]
21. Hagan, L.M.; McCormick, D.W.; Lee, C.; Sleweon, S.; Nicolae, L.; Dixon, T.; Banta, R.; Ogle, I.; Young, C.; Dusseau, C.; et al. Outbreak of SARS-CoV-2 B. 1.617. 2 (Delta) variant infections among incarcerated persons in a federal prison—Texas, July–August 2021. *Morb. Mortal. Wkly. Rep.* **2021**, *70*, 1349. [CrossRef]
22. MacIntyre, C.R.; Costantino, V.; Trent, M. Modelling of COVID-19 vaccination strategies and herd immunity, in scenarios of limited and full vaccine supply in NSW, Australia. *Vaccine* **2021**, *40*, 2506–2513. [CrossRef]
23. Jentsch, P.C.; Anand, M.; Bauch, C.T. Prioritising COVID-19 vaccination in changing social and epidemiological landscapes: A mathematical modelling study. *Lancet Infect. Dis.* **2021**, *21*, 1097–1106. [CrossRef] [PubMed]
24. McNamara, L.A.; Wiegand, R.E.; Burke, R.M.; Sharma, A.J.; Sheppard, M.; Adjemian, J.; Ahmad, F.B.; Anderson, R.N.; Barbour, K.E.; Binder, A.M.; et al. Estimating the early impact of the US COVID-19 vaccination programme on COVID-19 cases, emergency department visits, hospital admissions, and deaths among adults aged 65 years and older: An ecological analysis of national surveillance data. *Lancet* **2022**, *399*, 152–160. [CrossRef] [PubMed]
25. Choi, Y.; Kim, J.S.; Kim, J.E.; Choi, H.; Lee, C.H. Vaccination prioritization strategies for COVID-19 in Korea: A mathematical modeling approach. *Int. J. Environ. Res. Public Health* **2021**, *18*, 4240. [CrossRef] [PubMed]
26. Iboi, E.A.; Ngonghala, C.N.; Gumel, A.B. Will an imperfect vaccine curtail the COVID-19 pandemic in the US? *Infect. Dis. Model.* **2020**, *5*, 510–524. [PubMed]
27. Machado, B.; Antunes, L.; Caetano, C.; Pereira, J.F.; Nunes, B.; Patrício, P.; Morgado, M.L. The impact of vaccination on the evolution of COVID-19 in Portugal. *Math. Biosci. Eng.* **2022**, *19*, 936–952. [CrossRef]
28. Fisman, D.N.; Amoako, A.; Tuite, A.R. Impact of population mixing between vaccinated and unvaccinated subpopulations on infectious disease dynamics: Implications for SARS-CoV-2 transmission. *CMAJ* **2022**, *194*, E573–E580. [CrossRef]
29. Taboe, H.B.; Asare-Baah, M.; Yesmin, A.; Ngonghala, C.N. The impact of age structure and vaccine prioritization on COVID-19 in West Africa. *Infect. Dis. Model.* **2022**, *7*, 709–727. [CrossRef]
30. Zuo, C.; Meng, Z.; Zhu, F.; Zheng, Y.; Ling, Y. Assessing vaccination prioritization strategies for COVID-19 in south africa based on age-specific compartment model. *Front. Public Health* **2022**, *10*, 876551. [CrossRef]
31. Yang, C.; Yang, Y.; Li, Y. Assessing vaccination priorities for different ages and age-specific vaccination strategies of COVID-19 using an SEIR modelling approach. *PLoS ONE* **2021**, *16*, e0261236. [CrossRef]
32. Ackah, B.B.; Woo, M.; Stallwood, L.; Fazal, Z.A.; Okpani, A.; Ukah, U.V.; Adu, P.A. COVID-19 vaccine hesitancy in Africa: A scoping review. *Glob. Health Res. Policy* **2022**, *7*, 1–20. [CrossRef]
33. Mutombo, P.N.; Fallah, M.P.; Munodawafa, D.; Kabel, A.; Houeto, D.; Goronga, T.; Mweemba, O.; Balance, G.; Onya, H.; Kamba, R.S.; et al. COVID-19 vaccine hesitancy in Africa: A call to action. *Lancet Glob. Health* **2022**, *10*, e320–e321. [CrossRef] [PubMed]
34. Kanyanda, S.; Markhof, Y.; Wollburg, P.; Zezza, A. Acceptance of COVID-19 vaccines in sub-Saharan Africa: Evidence from six national phone surveys. *BMJ Open* **2021**, *11*, e055159. [CrossRef] [PubMed]
35. Clemens, J.; Aziz, A.B.; Tadesse, B.T.; Kang, S.; Marks, F.; Kim, J. Evaluation of protection by COVID-19 vaccines after deployment in low and lower-middle income countries. *EClinicalMedicine* **2022**, *43*, 101253. [CrossRef] [PubMed]

36. Rabiu, M.; Iyaniwura, S.A. Assessing the potential impact of immunity waning on the dynamics of COVID-19 in South Africa: An endemic model of COVID-19. *Nonlinear Dyn.* **2022**, *109*, 203–223. [CrossRef]
37. Choe, P.G.; Kang, C.K.; Suh, H.J.; Jung, J.; Song, K.H.; Bang, J.H.; Kim, E.S.; Kim, H.B.; Park, S.W.; Kim, N.J.; et al. Waning antibody responses in asymptomatic and symptomatic SARS-CoV-2 infection. *Emerg. Infect. Dis.* **2021**, *27*, 327. [CrossRef]
38. Goldberg, Y.; Mandel, M.; Bar-On, Y.M.; Bodenheimer, O.; Freedman, L.; Haas, E.J.; Milo, R.; Alroy-Preis, S.; Ash, N.; Huppert, A. Waning immunity after the BNT162b2 vaccine in Israel. *N. Engl. J. Med.* **2021**, *385*, e85. [CrossRef]
39. Tovissodé, C.F.; Doumatè, J.T.; Glèlè Kakaï, R. A Hybrid Modeling Technique of Epidemic Outbreaks with Application to COVID-19 Dynamics in West Africa. *Biology* **2021**, *10*, 365. [CrossRef] [PubMed]
40. Diekmann, O.; Heesterbeek, J.A.P.; Metz, J.A. On the definition and the computation of the basic reproduction ratio R 0 in models for infectious diseases in heterogeneous populations. *J. Math. Biol.* **1990**, *28*, 365–382. [CrossRef]
41. As, V.S.; Gribben, C.; Bishop, J.; Hanlon, P.; Caldwell, D.; Wood, R.; Reid, M.; McMenamin, J.; Goldberg, D.; Stockton, D.; et al. Effect of vaccination on transmission of COVID-19: An observational study in healthcare workers and their households. *N. Engl. J. Med.* **2021**, *21*, 2021–03.
42. Marks, M.; Millat-Martinez, P.; Ouchi, D.; h Roberts, C.; Alemany, A.; Corbacho-Monné, M.; Ubals, M.; Tobias, A.; Tebé, C.; Ballana, E.; et al. Transmission of COVID-19 in 282 clusters in Catalonia, Spain: A cohort study. *Lancet Infect. Dis.* **2021**, *21*, 629–636. [CrossRef]
43. Wang, Y.; Zheng, K.; Gao, W.; Lv, J.; Yu, C.; Wang, L.; Wang, Z.; Wang, B.; Liao, C.; Li, L. Asymptomatic and pre-symptomatic infection in Coronavirus Disease 2019 pandemic. *Med Rev.* **2022**, *2*, 66–88. [CrossRef]
44. Chen, X.; Huang, Z.; Wang, J.; Zhao, S.; Wong, M.C.S.; Chong, K.C.; He, D.; Li, J. Ratio of asymptomatic COVID-19 cases among ascertained SARS-CoV-2 infections in different regions and population groups in 2020: A systematic review and meta-analysis including 130, 123 infections from 241 studies. *BMJ Open* **2021**, *11*, e049752. [CrossRef] [PubMed]
45. Sobczak, M.; Pawliczak, R. COVID-19 vaccination efficacy in numbers including SARS-CoV-2 variants and age comparison: A meta-analysis of randomized clinical trials. *Ann. Clin. Microbiol. Antimicrob.* **2022**, *21*, 1–12. [CrossRef]
46. Jabłońska, K.; Aballéa, S.; Toumi, M. The real-life impact of vaccination on COVID-19 mortality in Europe and Israel. *Public Health* **2021**, *198*, 230–237. [CrossRef]
47. Musa, S.S.; Wang, X.; Zhao, S.; Li, S.; Hussaini, N.; Wang, W.; He, D. The heterogeneous severity of COVID-19 in African countries: A modeling approach. *Bull. Math. Biol.* **2022**, *84*, 1–16. [CrossRef]
48. COVID-19 Vaccination—Africa CDC. Available online: https://www.cdc.gov/media/releases/2021/s1119-booster-shots.html (accessed on 26 August 2021).
49. Onigbinde, O.A.; Ajagbe, A.O. COVID-19 vaccination and herd immunity In Africa: An incentive-based approach could be the game-changer to vaccine hesitancy. *Public Health Pract.* **2022**, *4*, 100282. [CrossRef]
50. Townsend, J.P.; Hassler, H.B.; Sah, P.; Galvani, A.P.; Dornburg, A. The durability of natural infection and vaccine-induced immunity against future infection by SARS-CoV-2. *Proc. Natl. Acad. Sci. USA* **2022**, *119*, e2204336119. [CrossRef]
51. Dan, J.M.; Mateus, J.; Kato, Y.; Hastie, K.M.; Yu, E.D.; Faliti, C.E.; Grifoni, A.; Ramirez, S.I.; Haupt, S.; Frazier, A.; et al. Immunological memory to SARS-CoV-2 assessed for up to 8 months after infection. *Science* **2021**, *371*, eabf4063. [CrossRef]
52. Curley, B. How long does immunity from COVID-19 vaccination last? Healthline. 2021. Available online: https://www.healthline.com/health-news/how-long-does-immunity-from-covid-19-vaccination-last (accessed on 25 July 2021).
53. Xin, H.; Li, Y.; Wu, P.; Li, Z.; Lau, E.H.; Qin, Y.; Wang, L.; Cowling, B.J.; Tsang, T.; Li, Z. Estimating the latent period of coronavirus disease 2019 (COVID-19). *Clin. Infect. Dis.* **2021**, *74*, 1678–1681. [CrossRef] [PubMed]
54. Mancuso, M.; Eikenberry, S.E.; Gumel, A.B. Will vaccine-derived protective immunity curtail COVID-19 variants in the US? *Infect. Dis. Model.* **2021**, *6*, 1110–1134. [CrossRef] [PubMed]
55. Parry, H.; Tut, G.; Bruton, R.; Faustini, S.; Stephens, C.; Saunders, P.; Bentley, C.; Hilyard, K.; Brown, K.; Amirthalingam, G.; et al. mRNA vaccination in people over 80 years of age induces strong humoral immune responses against SARS-CoV-2 with cross neutralization of P. 1 Brazilian variant. *Elife* **2021**, *10*, e69375. [CrossRef] [PubMed]